EFFECT OF MELANOIDINS AND METALS ON HYDROLYSIS IN ANAEROBIC DIGESTION

By

Sasha Sutaria

in partial fulfilment of the requirements for the degree of
MSc. in Environmental Engineering,
at Delft university of Technology,

Committee	:	Prof. Dr. Ir. Merle de Kreuk
		Prof. Dr. Ir. Jules van Lier
		Dr. Ir. Robbert Kleerebezem
Daily Supervisor	:	Javier Pavez Jara

Fall in love with the process and the results will come.

Anonymous

Acknowledgements

I would like to express my deepest appreciation to my daily supervisor, Javier Pavez Jara, for his knowledge, patience, time, encouragement and positive attitude. He has always been available to mentor me during the research process with a new insight and most importantly was always there to motivate me through the process of writing the report through the difficult times of COVID lockdown. I would always appreciate his honesty regarding my work which forced me push myself to work harder and better.

I would also like to thank the chair of my committee, Prof. Dr. Ir. Merle de Kreuk, for her valuable supervision and guidance throughout the thesis. I have always been inspired by her stories regarding her experiences during her PhD phase. It made me believe that with passion and hard work, one can overcome all problems and situations to move towards achieving greater things.

I would also like to thank Prof. Dr. Ir. Jules van Lier and Dr. Ir. Robbert Kleerebezem as part of my committee for providing recommendations, advice, and asking questions for better understanding during various meetings. I would not have imagined having a better committee than this one for my research at TU Delft. In addition, a special word of thanks to the lab technicians Armand Middeldorp and Patrica van den Bos.

Lastly, I would like to thank my parents for their continuous love and giving me the opportunity to study at TU Delft and encouraging me to aim high in life. A big thank you to my sister and all my friends for their constant support, encouraging words, opinions, and regular fun breaks from work which made my time at TU Delft memorable. I would also like to appreciate the support of my boyfriend without whom I would not have been at the finish line today.

Sasha Sutaria
Delft, 2020

Abstract

Sludge management has gained importance over the years due to high sludge treatment and disposal cost, stringent disposal laws, and a need to move towards sustainable energy production. Anaerobic Digestion (AD) of waste activated sludge (WAS) is a favoured sludge stabilisation technique due to its low energy footprint. Hydrolysis – the first step in AD is often the rate limiting step and thus pre-treatment such as Thermal Hydrolysis Process (THP) are implemented before AD to improve the biodegradability of WAS and biogas production. However, THP leads to the formation of recalcitrant compounds such as melanoidins which are presumed to have a similar effect as Humic substances on AD. Also, THP leads to the release of metals incorporated in sludge flocs by the degradation of extracellular polymeric substances (EPS) structures. Therefore, this study aimed to understand the effect of melanoidins and metals on the hydrolysis step in AD.

The interaction between melanoidins and cations Fe^{2+}, Ca^{2+}, Mg^{2+}, Cu^{2+}, K^{+}, and NH_4^{+} was studied using ultra-filtration and ICP-MS. The effect of these melanoidins-metals interactions on enzymatic hydrolysis of cellulose and proteins was investigated using fluorescence essay and Response Surface Methodology (RSM) modelling. The mechanism of inhibition of hydrolysis by melanoidins and metal was investigated using SEC-HPLC.

The results showed that complexation of melanoidins with metals shows the trend - $Fe^{2+} > Ca^{2+} > Mg^{2+} > Cu^{2+} > K^{+} \geq NH_4^{+}$. The ions with higher charge and ionic radius interacted with melanoidins more effectively. The melanoidins-metal interaction increased with an increase in melanoidins concentration most likely due to more phenolic and carboxylic functional groups available for binding. Fe^{3+} leads to an increase in molecular weight (MW) of melanoidins due to inter-molecular interaction caused by complete charge neutralisation, while no MW changes are observed with Cu^{2+} and Ca^{2+}. Individually, melanoidins decreased, Fe^{3+} increased, while Cu^{2+} decreased the rate of hydrolysis of cellulose. In the presence of melanoidins, the inhibiting effect of Cu^{2+} is decreased with increasing melanoidins concentration. Similarly, the positive effect of Fe^{3+} is decreased with increasing melanoidins concentration. Protein hydrolysis was completely inhibited with 3 mM metals concentration. Melanoidins and Fe^{3+} concentrations had no major impact on protein hydrolysis while Cu^{2+} inhibits hydrolysis even at 0.15 mM concentration.

Therefore, it was hypothesised that Cu^{2+} causes enzymatic inhibition, but in the presence of melanoidins, melanoidins-Cu^{2+} complexes formation mitigates the toxic effect of Cu^{2+} on hydrolysis thus improving the rate of hydrolysis. While, Fe^{3+} improved hydrolysis by facilitating substrate-enzyme interaction but in presence of melanoidins, melanoidins-Fe^{3+} complexation lead to non-availability of Fe^{3+} to facilitate hydrolysis process thus having no major impact on rate of hydrolysis.

List of Abbreviations

AD	:	Anaerobic Digestor
ANOVA	:	Analysis of variance
BOD	:	Biochemical oxygen demand
COD	:	Chemical oxygen demand
EPS	:	Extracellular polymeric substances
FA	:	Fulvic Acid
HA	:	Humic Acid
ICP-MS	:	Inductively coupled plasma mass spectrometry
MW	:	Molecular Weight
PS	:	Primary sludge
SEC-HPLC	:	Size exclusive chromatography-High performance liquid chromatography
SRT	:	Solids retention time
SS	:	Suspended solids
THP	:	Thermal Hydrolysis Process
TOC	:	Total organic carbon
TS	:	Total solids
UVA	:	Ultra-violet absorbance
VFA	:	Volatile fatty acids
VS	:	Volatile solids
WAS	:	Waste activated sludge
WWTP	:	Wastewater treatment plant

Contents

List of Tables

List of Figures

1

Introduction

1.1 Background knowledge

The secondary waste (such as sludges, sorting residues, and incineration ashes) generated from the Water and Waste sectors of Europe have increased by 38 % since 2010 (EEA, 2018). EU is moving away from landfilling of waste towards resource recovery, recycling, and incineration making the sludge disposal norms more stringent (EEA, 2018). Due to this increase in the production of sludge from Wastewater treatment plants (WWTPs) and stringent disposal laws, sludge management in WWTPs has gained importance over the years.

Sludge treatment and disposal cost around 50 – 60 % of the total operational cost of the WWTPs (Pilli et al., 2015; Ruffino et al., 2016). Therefore, to reduce the cost of disposal, meet the disposal regulations and reduce health associated problems, it is of utmost importance (i) to reduce the water content of the sludge, (ii) transform the organic matter into relatively stable or inert organic/ inorganic residue and (iii) condition the residue before disposal (Appels et al., 2008). Anaerobic Digestion (AD) is one of the favoured sludge stabilisation technique due to its low energy footprint.

AD is a microbiological process in which complex organic matter is converted to methane (CH_4) and carbon dioxide (CO_2) in the absence of oxygen via four sequential steps; hydrolysis, acidogenesis, acetogenesis, and methanogenesis (Metcalf & Eddy, 2014). This transformation of organic matter can reduce the amount of waste activated sludge (WAS) by 40–50 % while producing renewable energy in the form of biogas thus, optimising WWTP costs (Appels et al., 2008; S. Zhang et al., 2015). Other advantages of AD include the reduction of pathogens and reduction in odour-related problems.

AD is widely applied to primary sludge (PS) originating from primary treatment, WAS originating from biological treatment of the WWTP or mixes of both. PS constitutes 5-6 % dry solids and is mostly highly biodegradable organic matter. On the contrary, WAS has low biodegradability, as it consists of microbial cells agglomerated by extracellular polymeric substances (EPS) and cations resulting in compact flocs (Appels et al., 2008; Kuglarz et al., 2013; Traversi et al., 2015). Therefore, the application of AD for WAS is limited by low biodegradability, high retention times, and high reactor volumes requirements. For instance, in WAS originating from biological nutrient removal WWTP, only about 30–35% of the organic solids are anaerobically biodegradable in 20–25 days solids retention time (SRT) (Ruffino et al., 2016; Valo et al., 2004).

Hydrolysis - the conversion of carbohydrates, proteins, and lipids into lower molecular weight (MW) compounds such as sugars, amino acids, and fatty acids is widely regarded as the rate-limiting step of degradation of particulate organic matter in WAS (Pavlostathis & Gossett, 1986, 1988; Stuckey & McCarty, 1984; Vavilin et al., 2008). To overcome this drawback many pre-treatments for WAS have been developed which causes the lysis of cells in the sludge thus releasing and solubilising intracellular material into the liquid phase which increases biodegradability of sludge and biogas yield (Barber, 2016).

Various sludge pre-treatment techniques like thermal, chemical, mechanical, biological, physical and combinations of these are developed (Weemaes & Verstraete, 1998). Thermal Hydrolysis Process (THP) is a well-established and commercially implemented technology prior to AD. In this process, the temperature and pressure of sludge are increased to improve its biodegradability in AD. Several advantages of THP are the increase in methane production in AD, increase in dewaterability, destruction of pathogens, lower transportation costs due to lower residual sludge after AD and production of class-A bio-solids (Bougrier et al., 2008; Climent et al., 2007; Kepp et al., 2000; Neyens & Baeyens, 2003; Valo et al., 2004).

However, due to the application of THP, an increase in recalcitrant compounds such as melanoidins has been observed in AD (Bougrier et al., 2008; Liu et al., 2012; Stuckey & McCarty, 1984). Melanoidins are brown Humic Acid (HA) like compounds formed by Millard reaction at higher temperatures (Blondeau, 1989; Martins et al., 2000). The amount of melanoidins produced increases with an increase in process temperature (Dwyer et al., 2008). Formation of these humic-like compounds might lead to inhibition of hydrolysis and increased colour production in AD and AD reject water (Brons et al., 1985; Butler & Ladd, 1971; T. V. Fernandes et al., 2015).

Also, in the THP process, heavy metals and trace elements that are incorporated in sludge flocs by adsorption to EPS matrix, ware released to the liquid phase due to degradation of EPS structures with an increase in temperature (Appels et al., 2010; Veeken & Hamelers, 1999). Moreover, at high temperatures, the solubilisation of metals is enhanced because the diffusivity of ions is promoted (Dewil et al., 2007). An increase in energy applied to WAS and solubilisation of organic matter, lead to an increase in soluble concentrations of Ca^{2+} and Mg^{2+}. (Laurent et al., 2009).

The increase in melanoidins and metals concentration during THP is thought to affect the digestion of sludge. Therefore, this study aims at providing a better understanding on the effect of melanoidins and metals on hydrolysis step in AD.

1.2 Research Scope

Previous research has shown that the presence of humic substances inhibits hydrolysis in AD. Fernandes et al. (2015) extracted humic and fulvic compounds from cow manure and maize silage to test their inhibitory potential on anaerobic cellulose and tributyrin degradation in batch incubations. Consequently, to mitigate the inhibition by HAs, the addition of excess amounts of hydrolytic enzymes was proposed (Fernandes et al., 2015). Also, Brons et al. (1985) showed that the addition of Ca^{2+} cations reversed the inhibitory effects of humate on potato protein hydrolysis. More recently, Azman et al. (2015) studied the mitigation of HA inhibition on anaerobic cellulose digestion by adding several metal salts such as Ca^{2+}, Fe^{3+}, Na^{+}, K^{+}, Mg^{2+} in a batch test. This research was carried out with granular, methanogenic sludge (Azman et al., 2015). It was found that the hydrolysis efficiency was improved by 44 %, 32 %, and 40 % by addition of 5mM Ca^{2+}, Mg^{2+} ,and Fe^{3+} respectively along with HAs (Azman et al., 2015).

However, the aim of the studies conducted till date was to find the mitigating potential of metals on the inhibiting effect of HA on hydrolysis and therefore the concentrations of metals used were as high as 5mM or 10mM. This study focuses on conducting the test with concentrations of metals commonly found in an AD after THP and thus provide a better insight into the mechanism of hydrolysis in the presence of melanoidins and metals. The previous studies are conducted with HAs derived by different

extraction methods and from different sources which might have different effects on AD (Fernandes, 2010). In this research laboratory prepared melanoidins are used to provide consistency in all the tests and to access if humic-like melanoidins show a different effect on hydrolysis than HAs due to differences in structure, functional groups, or charge.

Therefore, this thesis investigates the effect of melanoidins and metals on the hydrolysis step in AD. In this study, it is hypothesised that "melanoidins bind to the active sites of enzymes, inhibiting the hydrolytic activity. In the presence of metals, melanoidins-metal complexes are formed thus reducing the binding capacity of melanoidins to enzymes and increasing the rate of hydrolysis ". The research is conducted by answering three questions individually:

1. What is the extent of melanoidins and metals interaction?
    - Metals potassium (K^{+}), calcium (Ca^{2+}), magnesium (Mg^{2+}), copper (Cu^{2+}), iron (Fe^{3+} or Fe^{2+}) and ammonium (NH_4^{+}) which are commonly found in AD are tested for interaction with melanoidins. However, copper and iron could also be found in their reduced form Cu^{+1} and Fe^{2+} respectively depending on the reactor conditions.
2. What is the effect of the presence of melanoidins and metals on the rate of hydrolysis of cellulose and proteins?
    - The metals which show maximum interaction with melanoidins are further tested. The hydrolysis test is conducted in a batch for cellulase and protease activity.
3. What is the mechanism in which melanoidins interfere? Do melanoidins bind to the active sites of enzymes and does the presence of metals decrease this binding by melanoidins and metals interaction?
    - Tests were conducted with enzyme cellulases and metals Cu^{2+} and Fe^{3+} to prove or disprove the hypothesis stated in the thesis.

1.3 Thesis Outline

The thesis starts by providing a short background on the importance of AD in WAS treatment and the merits and demerits of THP process applied prior to AD. Along with this, the research objectives are explained in **chapter 1**. In **chapter 2** available scientific knowledge on THP and AD are reviewed. Special emphasis is given to the hydrolysis of cellulose and proteins - its mechanism, limiting factors, and kinetics as it is the focus of the study. **Chapter 3** describes the research method and analysis techniques applied in this study. **Chapter 4** provides the results obtained for the research questions separately and a possible mechanism of hydrolysis in the presence of melanoidins and metals is discussed. The results are discussed taking into consideration other such similar research conducted. **Chapter 5** presents the limitation of this study and recommendations for further research while **Chapter 6** provides the conclusion of this research.

2

Literature review

2.1 Anaerobic Digestion

AD of complex organic matter is a four-step complex process that converts degradable organic compounds to methane (CH_4) and carbon dioxide (CO_2) in the absence of elemental oxygen. These four stages of AD are hydrolysis, acidogenesis, acetogenesis, and methanogenesis as shown in Figure 1. Hydrolysis - the first step, is the breakdown of complex high molecular weight substrates such as carbohydrates, lipids, proteins to soluble organic substances such as sugars, amino acids, long-chain fatty acids (LCFA), glycerol by exo-enzymes secreted by hydrolytic and fermentative bacteria (Appels et al., 2008).

The second step - acidogenesis is where dissolved compounds produced during hydrolysis enter the cells of fermentative bacteria and are converted to volatile fatty acids (VFAs), alcohols, NH_3, H_2, CO_2, and H_2S and then excreted from the cells (van Lier et al., 2008). The third step - acetogenesis is the anaerobic conversion of VFAs and alcohols produced in the acidogenesis step into acetate, H_2, and CO_2 by acetogenic bacteria. The most common acetogenic substrates are propionate and butyrate - key intermediates in the AD process (van Lier et al., 2008).

Methanogenesis is the final step in AD where acetate, H_2, and CO_2 are converted to gaseous CH_4 and CO_2. This step is accomplished by two groups of bacteria – acetotrophic methanogens and hydrogenotrophic methanogens. Acetotrophic methanogens decarboxylate acetate to form CH_4 while hydrogenotrophic methanogens reduce CO_2 using H_2 as an electron donor (van Lier et al., 2008).

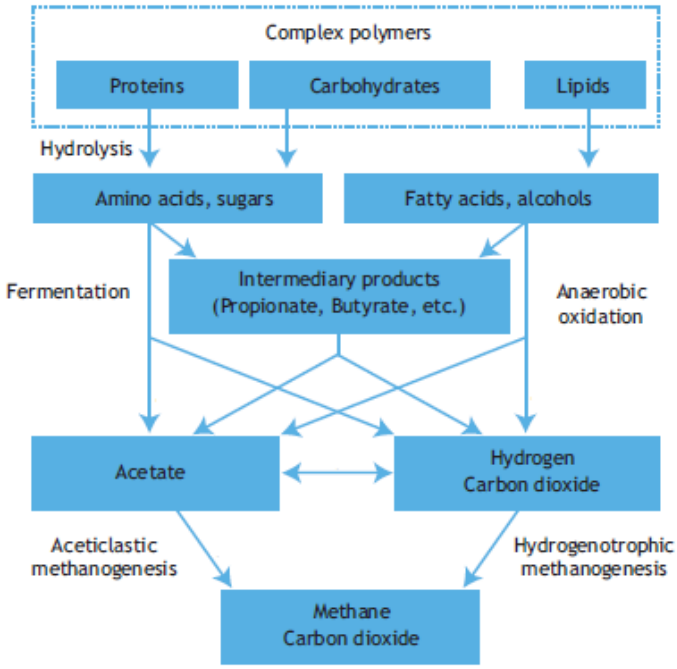

Figure 1: Anaerobic Digestion process (Gujer & Zehnder, 1983; van Lier et al., 2008)

2.2 Thermal Hydrolysis Process

High temperature thermal hydrolysis involves the application of temperature above 100°C prior to the AD of PS or WAS or mixer of both which leads to sludge solubilisation and improved sludge biodegradability. THP is more suited for WAS as it consists of 10-24% of bacterial biomass which is difficult to break down anaerobically, 7-19% carbohydrates and 25-62 % proteins which are mostly surrounded by a cell membrane and cell wall which acts as a strong barrier to hydrolytic enzyme penetration thus limiting the efficacy of the biological process (Gonzalez et al., 2018; Ruffino et al., 2016; Stuckey & McCarty, 1984; Traversi et al., 2015).

In THP, the temperature of WAS is increased in the range of 160–180°C by either direct steam injection or by passing the steam through heat exchangers (Pilli et al., 2015, Bougrier et al., 2007; Haug et al., 1978; Y. Y. Li & Noike, 2015; Neyens & Baeyens, 2003; Stuckey & McCarty, 1984). Steam injection and increase in temperature together lead to an increase in pressure of the system to 6-25 bar (Weemaes & Verstraete, 1998). This pressure and temperature are maintained for 30 to 60 min and suddenly released, which causes the cells in the WAS to rapture thus solubilising intracellular material into the liquid phase and increasing biodegradability of WAS (Barber, 2016). It further leads to improved biogas production, improved dewaterability, reduced viscosity, and provides pathogen-free biosolids (Barber, 2016).

Some of the full-scale installations of THP are CambiTHP® by Cambi, Bio Thelys™ by Veolia Water Solutions and Technologies, TurboTec by Sustec BV, and LYSOTHERM® by Eliquo Water & Energy BV. CambiTHP® and Bio Thelys™ are most widely used commercial batch THP installations in Europe where the sludge is heated prior to AD by steam injection at a temperature of 140-165°C at 6 bar for 20-30 min in case of CambiTHP® while at 165°C at 9 bar for 30 min in case of Bio Thelys™ (Pilli et al., 2015). A detailed description of these processes is provided by Pilli et al. (2015).

2.2.1 Effect of THP on WAS

2.2.1.1 Solubility of Metals

Appels et al. (2010) studied the influence of low temperature THP of sludge on the solubilisation of various heavy metals such as cadmium, chromium, mercury, lead, copper, zinc, and nickel. The results indicated a linear increase in soluble metals concentration with energy supplied. Cu concentrations increased by 6-fold while Cr concentrations increased by 2-fold after treatment at 90°C for 60 min (Appels et al., 2010). Laurent et al. (2009) and Kuglarz et al. (2013) made a similar observation regarding concentrations of heavy metals, Ca^{2+} ,and Mg^{2+} which increased with increasing sonication energy and microwave energy provided to the WAS.

The extraction of heavy metals incorporated in the sludge flocs to the aqueous phase is enhanced at high temperatures as the rate of diffusion of ions is promoted at elevated temperatures (Veeken & Hamelers, 1999). Moreover, heavy metals are incorporated into the EPS of the sludge flocs and in the intracellular structures of the sludge micro-organisms. THP leads to the degradation of EPS, which releases heavy metals that are bound on these EPS in the sludge liquid phase (Dewil et al., 2007).

2.2.1.2 Solubility of carbohydrates and proteins

Solubilisation here is the transfer of carbohydrates and proteins from a particulate fraction of WAS to the soluble fraction of WAS. Bougrier et al. (2008) observed a linear increase in solubility of carbohydrates in WAS between temperature 90-130°C, while solubility of proteins was found to

increase steeply between temperatures 130-170°C. It was hypothesised that carbohydrates were mainly located in the exopolymers of sludge structure which were affected by lower temperatures, whereas proteins were mainly located inside the cells which were solubilised at higher temperatures when cell walls were lysed (Bougrier et al., 2008). The same was confirmed by the studies of Liu et al. (2012), where carbohydrates and proteins in soluble phase of WAS increased after thermal hydrolysis at 175°C for 60 min. The increase in solubility with MW > 300kDa, which accounted for biopolymer release due to cell wall rapture was found to be higher in proteins than in carbohydrates (Liu et al., 2012).

Wilson & Novak, (2009) observed that carbohydrates were only solubilized and not degraded to mono or dimeric sugar units between temperature 130-220°C. Extensive protein degradation was not observed at temperatures below 170°C, but proteins denaturation and degradation were observed with an increase in ammonia concentration after THP between 190-220°C. (Bougrier et al., 2007; Wilson & Novak, 2009).

It is hypothesized that at temperatures higher than 150°C, soluble carbohydrates reacted with themselves or with soluble proteins to form organic compounds which were like Amadori compounds or melanoidins which leads to brown coloured supernatant after THP (Bougrier et al., 2008; Dwyer et al., 2008; Wilson & Novak, 2009).

2.2.1.3 Anaerobic Biodegradability of WAS

For temperatures lower than 200°C, COD solubilisation in WAS was found to increase with temperature (Bougrier et al., 2008; Haug et al., 1978; Valo et al., 2004). THP of WAS at 175°C increased methane production by 35 % (Liu et al., 2012) and 27 % (Stuckey & McCarty, 1984) over the control. It is also suggested that AD following THP are optimized at a retention time of 10 to 12 days as approximately 95 % of biogas potential can be realised by 20 days. (Xue et al., 2015). The maximum degradability of organic matters and methane production in AD was found around temperatures 170 - 190°C even though COD solubilization continues to increase in proportion to temperatures up to 220 °C (Bougrier et al., 2007, 2008; Y. Y. Li & Noike, 2015; Stuckey & McCarty, 1984).

According to Stuckey & McCarty (1984), the observed peak in methane production could be caused by two competing mechanisms: cell lysis and the conversion of particulate organics into the biodegradable dissolved matter, which increases methane yield; and the formation of soluble organic but refractory compounds such as melanoidins that do not contribute to biogas production. As the solubility of sugars and proteins increases at temperatures above 140°C, higher production of melanoidins is observed above this temperature (Bougrier et al., 2008; Liu et al., 2012; Stuckey & McCarty, 1984).

2.2.1.4 Production of Refractory compounds - Melanoidins

Melanoidins are brown, high MW heterogeneous polymers formed due to Millard reaction - a non-enzymatic chemical reaction between amino acids and reducing sugars (Martins et al., 2000). Due to their recalcitrant nature, melanoidins are also known as synthetic Humic Acid (HAs) (Blondeau, 1989).

The Maillard reaction can be divided into three stages: early, advanced, and final which can occur simultaneously and are interrelated as shown in Figure 2 (de Oliveira et al., 2016). The first stage is the condensation of the carbonyl group of reducing sugar with a compound containing a free amino group

to produce N-substituted glycosilamine and water. The unstable glycosilamine undergoes Amadori re-arrangement forming ketosamines.

In the advanced stage, the ketosamines further react depending on the pH. At pH ≤ 7, furfural (when pentoses are involved) or hydroxy-methyl furfural (when hexoses are involved) are formed. At pH > 7 the degradation of the Amadori compound is thought to produce two water molecules and reductones or a variety of short-chain hydrolytic fission products (Martins et al., 2000). All these compounds are highly reactive and take part in further reactions. Carbonyl groups can condense with free amino groups, which results in the incorporation of nitrogen into the reaction products. Di-carbonyl compounds react with amino acids with the formation of aldehydes and aminoketones known as the Strecker degradation (Martins et al., 2000).

Subsequently, in a final stage, a range of reactions takes place such as cyclization, dehydration, rearrangement, isomerization, condensation which ultimately leads to the formation of brown nitrogenous polymers and co-polymers known as melanoidins (Martins et al., 2000).

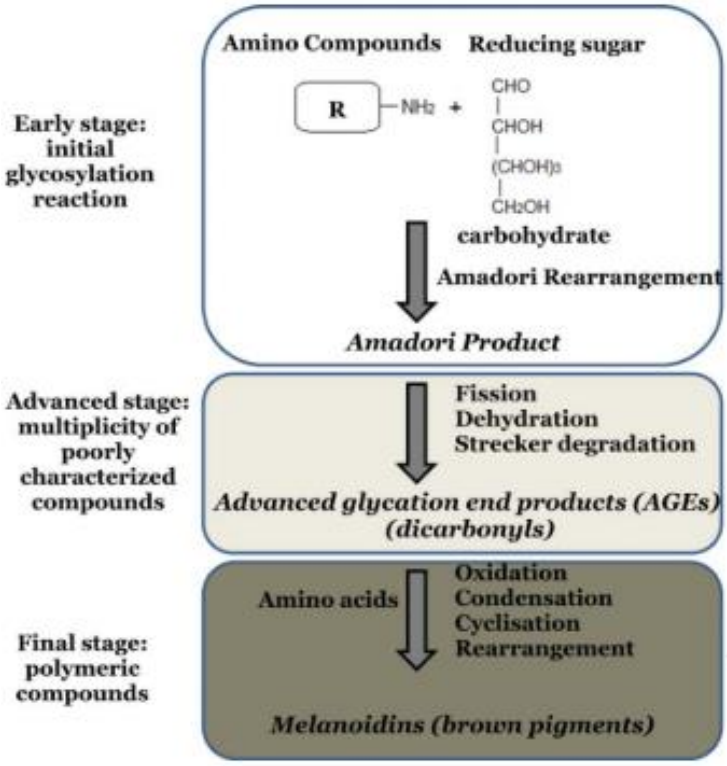

Figure 2: Stages of the Maillard reaction (de Oliveira et al., 2016)

Bougrier et al. (2007) observed that though the concentration of soluble proteins increased to 52 % of the total proteins after THP at 190°C against 32 % in control, the soluble protein removal yield in AD was decreased to 68% after THP at 190°C against 75% in the control. This was probably due to the formation of melanoidins with soluble proteins. This phenomenon of decreased protein removal yield was not shown for THP at 135°C. Thus, melanoidins production was observed for THP temperatures higher than 135°C (Bougrier et al., 2007). Dwyer et al. (2008) showed that the colour produced in the effluent of THP was due to melanoidins production and by decreasing the THP operating temperatures from 165°C to 140°C, the colour in the effluent of THP could be reduced by 70 % with no significant decrease in biodegradability of WAS. Thus, at temperatures higher than 190°C, the formation of

melanoidins outcompetes the formation of biodegradable soluble components, thereby reducing biodegradation. The exact temperature, however, depends on sludge composition, and probably other factors (Gonzalez et al., 2018).

2.3 Hydrolysis

Hydrolysis is defined as a process in which complex polymeric substrates - particulate or dissolved are degraded through the action of exo-enzymes secreted by hydrolytic and fermentative bacteria to produce monomeric or dimeric compounds which can easily cross the cell membrane of obligate anaerobic acidogenic bacteria (Gallert & Winter, 2008; van Lier et al., 2008).

Enzymes are proteinaceous molecules that catalyse biochemical reactions. They can be divided into two types: endo-enzymes (function within the cell) and exo-enzyme (function outside the cell) (Gerardi, 2003). The catalytic mechanism can be represented as a "lock-and-key model" - the substrate molecule match perfectly with the active enzyme site allowing for the chemical reaction (Fischer, 1894, as cited in Sanders, 2001). This theory was later replaced by an "induced-fit model" – a substrate can cause changes in the protein structure bringing catalytic groups in the proper orientation for a reaction whereas a non-substrate will not (Koshland, 1958). The enzymes cellulases and amylases hydrolyse carbohydrates, proteases hydrolyse proteins and lipases and phospholipases hydrolyse lipids (Gallert & Winter, 2008).

Batstone et al., (2000) mentions that the release of enzymes by acidogenic bacteria and its further attachment to the substrate can be described by two main mechanisms:

1. Exo-enzymes secreted by acidogenic bacteria to the bulk liquid are adsorbed to particulate or dissolved substrate (Jain et al., 1992)
2. Acidogenic bacteria attach to the particulate substrate and secrete exo-enzymes. Soluble products are then directly utilised by these bacteria (Vavilin et al., 1996).

Irrespective of the used mechanism, it is postulated that acidogenic bacteria always produce excess enzymes thus achieving full colonisation of all available surface of the substrate. (Hobson, 1987). Therefore, the rate of hydrolysis of the particulate substrate is mostly dependent on particle size of the substrate or the number of adsorption sites at the substrate surface rather than the bacteria concentration (Hills & Nakano, 1984; Veeken & Hamelers, 1999). Hydrolysis is considered the rate-limiting step in the AD of particulate substrate or WW with high SS/COD ratio (Eastman & Ferguson, 1981; Zeeman et al., 1997). However, when digesting a concentrated substrate such as vegetable, fruit and yard waste with 35-40% total solids the diffusion rates of a substrate may become the rate-limiting step (Veeken & Hamelers, 1999).

In digestion of WAS, hydrolysis of sludge is preceded by death and lysis of biomass (Pavlostathis & Gossett, 1986). Pavlostathis & Gossett (1988) studied the digestion of WAS and autoclaved WAS which bypasses the lysis step and found that autoclaving leads to a 29 % increase in the ultimate digestibility of WAS. However, the effluent of the digester still consisted particulate proteins which accounted for 80 % of the total effluent degradable COD suggesting that hydrolysis was the rate limiting step rather than cell death/lysis (Pavlostathis & Gossett, 1988).

2.3.1 Enzymatic hydrolysis of Carbohydrates

Carbohydrates are a biomolecule consisting of carbon, hydrogen, and oxygen atoms. They are granules or fibres of varying sizes made of homo- or heteropolymers of hexoses, pentoses, or sugar derivatives which are mostly insoluble in water (Gallert & Winter, 2008). They can be divided into monosaccharides, disaccharides, oligosaccharides, and polysaccharides. Polysaccharides are a chain of many sugar monomers bound by glycosidic bonds (Gerardi, 2003).

Cellulose is a polysaccharide consisting of a linear chain of several hundred to thousands of d-glucose units linked by β-1,4 bonds. The hydrolysis of cellulose is performed by cellulases that hydrolyse β-1,4 linkages in cellulose chains. Cellulases are produced by a large diversity of microorganisms including both fungi and bacteria which can be aerobic, anaerobic, mesophilic or thermophilic. Cellulose and starch-degrading bacteria are found within the genera *Acetivibrio*, *Butyrivibrio*, *Caldanaerobacter*, *Caldicellulosiruptor*, *Clostridium, Eubacterium*, *Halocella*, *Ruminoclostridium* and *Ruminococcus* (phylum Firmicutes), *Bacteroides* and *Paludibacter, etc* (Westerholm & Schnürer, 2016).

The complete hydrolysis of cellulose is mediated by a combination of three main types of cellulases: First, endo-glucanase randomly attacks the internal β-1,4 glucosidic bonds resulting in glucan chains of different lengths. Subsequently, these oligosaccharides are hydrolysed by exo-glucanase from its reducing and non-reducing chain ends to produce cellobiose. Lastly, cellobioses or β-glucosidases hydrolyses the exo-glucanase product into individual monosaccharides. Figure 3 shows the described mechanism of hydrolysis of cellulose. (Mojsov, 2016; Pino et al., 2018; Sanders, 2001).

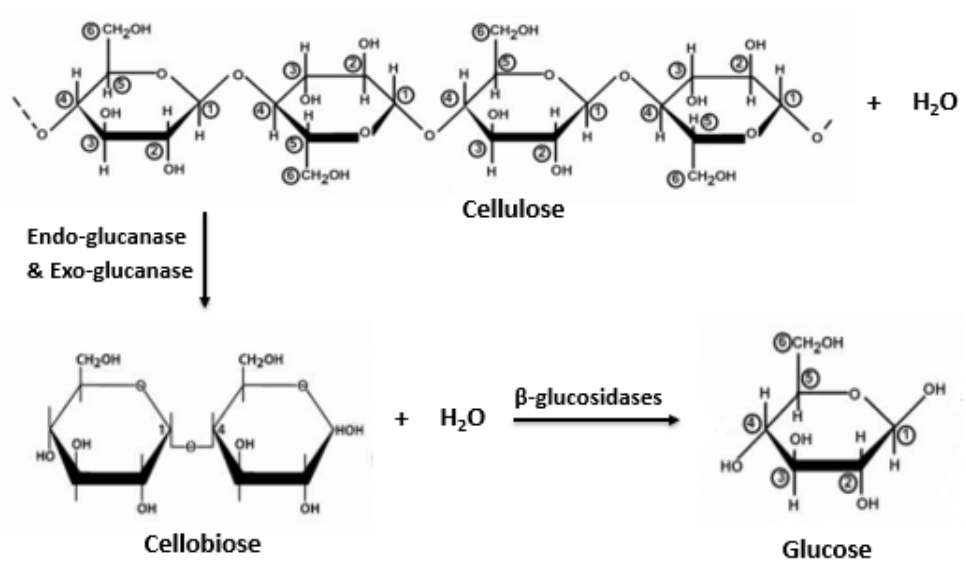

Figure 3: Hydrolysis of cellulose by cellulases adapted from (Pino et al., 2018)

2.3.2 Enzymatic hydrolysis of Proteins

Proteins are polymers composed of linear chains of amino acids linked by peptide bonds. Amino acid has a common carbon atom which is attached to a hydrogen atom, an amino group (NH_2), a carboxyl group (COOH), and a side chain (which could be hydrophobic, polar or charged group) specific to each amino acid. Peptide bonds are formed when the carboxyl group of one amino acid condenses with the amino group of next to release water molecules (Branden & Tooze, 1999). Protein structure is divided into four levels:

1. Primary Structure refers to the sequence of amino acids in a polypeptide chain. The ends of the polypeptide chains are carboxyl terminus (C^-) and amino terminus (N^-).
2. Secondary Structure is defined by the patterns of hydrogen bonds between the main-chain peptide groups. The side chains are not involved in the hydrogen bonding, but they do determine the type and stability of the structure. α-helix and β-sheets are the two main types of secondary structures (J. W. Pelley, 2007).
3. Tertiary structure is the three-dimensional structure of a protein formed spontaneously and stabilized both by side chain interactions and, in extracellular proteins by disulphide bonds. This folding brings distant sequences in a linear polypeptide together into a stable structure. The two main classes are fibrous and globular proteins. Fibrous proteins are generally composed of long, narrow strands of repetitive amino acid sequence while globular proteins are generally more compact and rounded in shape with an irregular amino acid sequence (Godbey, 2014; J. W. Pelley, 2007).
4. Quaternary structure is the three-dimensional structure consisting of the aggregation of two or more individual polypeptide chains (subunits) that operate as a single functional unit.

Proteases are enzymes that catalyse the hydrolysis of peptide bonds in proteins to smaller peptides and free amino acids as presented in Figure 4 (Haq et al., 2004). These enzymes are found in a wide diversity of sources such as plants, animals, and microorganisms but they are mainly produced by bacteria and fungi (Mojsov, 2016). Protein and amino acid degradation in anaerobic digesters have been performed by various genera within the phylum Firmicutes, such as *Anaeromusa*, *Aminobacterium*, *Aminomonas*, *Gelria*, *Peptoniphilus*, *Thermanaerovibrio*, *Clostridium*, *Proteiniborus*, and *Sporanaerobacter* (Westerholm & Schnürer, 2016).

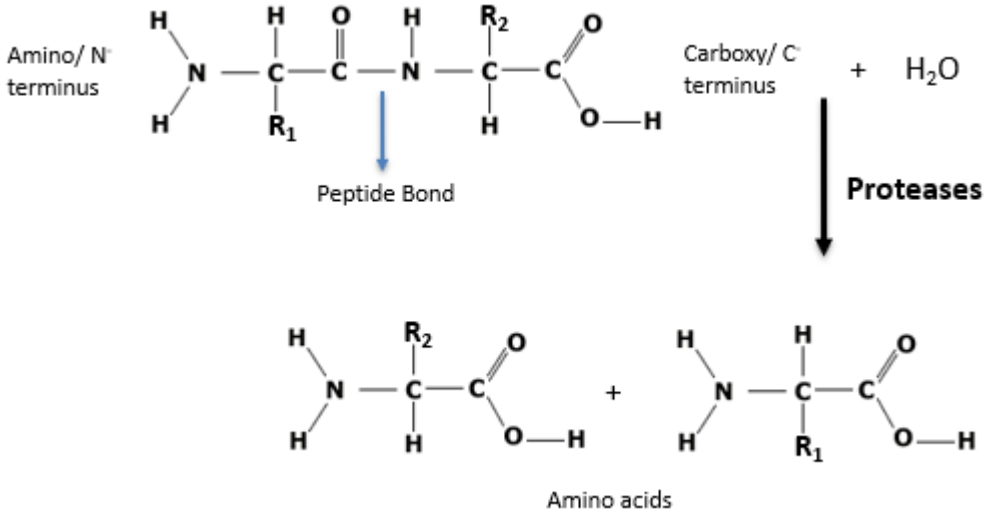

Figure 4: Hydrolysis of protein by proteases adapted from (Fernandes, 2010)

2.3.3 Factors affecting Hydrolysis

2.3.3.1 Temperature

Most of the anaerobic reactors are operated at either mesophilic (35-45°C) or thermophilic (45-60°C) conditions. Thermophilic microorganisms are more susceptible to temperature changes than mesophilic microorganisms and thus, for optimal biogas generation, the temperature fluctuations in

the thermophilic range should not exceed ±1°C, while in the mesophilic range this limit is ±3°C (Azman, 2016).

Hydrolysis by microbial enzymes has an optimum temperature range of 30°C to 60°C generally (Jonke & Michal, 2007). As per the studies of Veeken & Hamelers (1999), when the enzyme concentration is not rate-limiting, the relationship between temperature and hydrolysis rate can be expressed by Arrhenius equation with an activation energy of 64 ± 14 kJ mol^{-1} which is typical for enzyme kinetics (Veeken & Hamelers, 1999). It is indicated that an increase in temperature up to the optimum leads to an increase in the kinetic energy of the reactants, thus increasing the rate of reaction. Further increase in temperature leads to changes in the tertiary structure of enzymes resulting in thermal denaturation decreasing the rate of reaction and finally inactivating the enzyme (Jonke & Michal, 2007).

2.3.3.2 pH

The selection of operational pH for AD is rather complex, as the optimum pH for the growth of each microbial group in AD is different. Most hydrolytic microorganisms have an optimum pH between 5 and 7, whereas methanogen's growth is optimum at pH between 6.5 and 8.5 (Azman, 2016; Jonke & Michal, 2007). The optimum pH for an enzyme lies somewhere between the pKa values of two or more catalytic amino acids. Any decrease or increase in optimum pH can lead to protonation or ionization of these catalytic amino acids thus reducing or stopping the activity of the enzyme (Whiteley & Lee, 2006).

Hu et al. (2005) studied the effect of pH between 5.5 to 7.5 on cellulose degradation in AD by rumen microbes and concluded that a pH of 6 or above should be maintained to achieve optimal cellulose hydrolysis as at pH 5.5 there was no degradation while degradation increased with pH from pH 6.0 to 7.5. When Zhang et al. (2005) carried out anaerobic hydrolysis of protein and lipids rich kitchen waste at pH 5, 7, 9 and 11, it was found that at a pH of 7 82% of COD was solubilised and maximum VFA concentrations were achieved thus providing optimum working conditions for AD of kitchen waste at pH 7. Also according to the overview of Gallert & Winter (2008), anaerobic hydrolysis of carbohydrates is favoured at slightly acidic pH while proteins hydrolysis are stimulated at neutral or even slightly alkaline pH.

2.3.3.3 Humic and Fulvic acids

HAs are fractions of Humic substances which are soluble in alkaline media, partially soluble in water and insoluble in acidic media. The various functions of HAs are mainly attributable to the phenol and carboxylic acid functional groups, which allow the deprotonation of OH/OOH (Stevenson, 1994).

Brons et al. (1985) found that hydrolysis of potato protein was inhibited by the presence of HAs. HAs delayed hydrolysis but the rate of hydrolysis after the completion of the lag phase was similar to that without HAs. However, Jahnel & Frimmel (1994) studied the effect of humic substances isolated from different origins on the Pronase E activity and concluded that the rate of hydrolysis decreases in the presence of humic substances.

Fernandes et al. (2015) studied the effect of HAs extracted from cow manure and maize on enzymatic and microbially catalysed cellulose hydrolysis. The results showed that at HA concentration of 5 g/L, hydrolysis was completely inhibited in both trials, while at 0.5 g/L slow hydrolysis took place in microbially catalysed trails. Although inhibition mechanisms are not fully understood, a hypothesis

was presented - In enzymatic hydrolysis trials, cellulose hydrolysis did not take place probably because all enzymes added were bond to the functional groups of the HAs, while in microbially catalysed hydrolysis trials cellulose was hydrolysed at low concentrations of HAs probably because the acidogenic bacteria kept on secreting enzymes to hydrolyse the cellulose even though part of the enzymes were bond to the HAs, the excess of enzymes was able to hydrolyse the cellulose (T. V. Fernandes et al., 2015).

Further, some research has been done on mitigation of the inhibiting effect of HAs on hydrolysis. Ladd & Butler (1970) studied the impact of Mg^{2+} and K^{+} on hydrolysis by various proteases and concluded that divalent cations are more effective than monovalent cation in mitigating the inhibiting effect of HAs on hydrolysis. Ladd & Butler (1970) explained this inhibition and its mitigation by a simple explanation “humic acids reversibly bind enzymes by a cation-exchange mechanism causing inhibition or stimulation of enzymic activity and inorganic cations in sufficiently high concentrations displace the enzymes from the complexes “. Similar studies on mitigating the effect of adding metal salts Ca^{2+}, Fe^{3+}, Na^{+}, K^{+}, Mg^{2+} on HAs inhibition on cellulose digestion were conducted by Azman et al., (2015) with granular methanogenic sludge. It was found that the hydrolysis efficiency was improved by 44 %, 32 %, and 40 % by addition of 5mM Ca^{2+}, Mg^{2+}, and Fe^{3+} respectively along with HAs (Azman et al., 2015).

2.3.4 Kinetics of Hydrolysis

Kinetic models help to explain the behaviour of hydrolysis quantitatively and can provide useful information for the design and operation of the hydrolysis process and thus AD. Different mathematical models such as first-order kinetics, Michaelis-Menten kinetics, surface-based kinetics have been used in literature to describe the rate of hydrolysis depending on the type of substrate, biomass concentration or enzyme activity used in the study (Vavilin et al., 2008).

The most commonly used relation is an empirical first-order relation. Eastman & Ferguson (1981) developed an acid phase model wherein hydrolysis is considered only the conversion of particulate COD into soluble COD. Then, the hydrolysis rate at a constant temperature and pH is approximately first-order with respect to the remaining concentration of degradable particulate COD (Eastman & Ferguson, 1981).

In the surface-based hydrolysis models, it is assumed that enzyme activity is present in excess for the digestion of particulate substrates and that the hydrolysis rate depends on the amount of surface available for the hydrolytic enzymes (Hobson, 1987; Vavilin et al., 1996). The rate of hydrolysis depends on the size and shape of the particulate matter. Large particles with a low surface-to-volume ratio are hydrolysed more slowly layer by layer than small particles (Hills & Nakano, 1984; Hobson, 1987).

Michaelis-Menten kinetics is commonly used to describe the rate of the hydrolysis of dissolved polymeric substrates (Vavilin et al., 1996). In these models, enzyme concentration is considered to be limiting and therefore, the rate of hydrolysis depends not only on the remaining degradable COD but also on the concentration and activity of the hydrolytic enzymes or the hydrolytic biomass (Batstone et al., 2000; Goel et al., 1998a; Jain et al., 1992; Vavilin et al., 1996).

The model proposed by Goel et al. (1998a) for the hydrolysis of soluble starch showed that the rate of starch degradation was linearly dependent on the biomass concentration and the initial starch concentration as presented in equation 1. Further, Goel et al. (1998b) observed that enzyme activity in the cell-free fraction of WAS, was small compared to enzyme activity in the fraction with cells,

indicating that major activity of the hydrolytic enzymes is associated with the cell or lies within the EPS matrix of the flocs. This immobilization of enzyme activity by the EPS matrix of the flocs allows microorganisms not to have to waste energy in replenishing the enzyme pool continuously. Therefore, the sludge concentration and enzyme activity can be considered as interchangeable parameters in the case of WAS (Goel et al., 1998a, 1998b).

$$\frac{dS}{dt} = K_h \frac{S}{K_x + S} X \qquad \text{Eq. 1}$$

with:
S - Starch concentration (mg starch/L)
X - Biomass concentration (mg MLSS/L)
K_x - half-rate constant (mg starch/L)
K_h - maximum hydrolysis rate constant (mg starch/mg MLSS * d)

Jain et al. (1992) developed a model for the hydrolysis of cattle dung in which the hydrolysis was considered as a multi-step process including enzyme production, transfer of enzyme from microbe to bulk solution, and reaction with the substrate. A modified Michaelis-Menten equation was used to find the slowest stage in hydrolysis. Mass transfer of hydrolytic enzyme from microbe to bulk was the rate-controlling step in this stage which reduced the Michaelis-Menten equation to first order in bulk enzyme concentration and zero-order in substrate concentration (Jain et al., 1992).

2.4 Conclusion

From the literature survey presented in this chapter, it can be concluded that AD is one of the important sludge treatment technology and hydrolysis is a crucial step in the AD of WAS. THP of WAS leads to an increase in solubility of COD, carbohydrates and proteins, solubility of metals, biodegradability of WAS, and thus biogas production. However, it also leads to the formation of recalcitrant compounds such as melanoidins which are considered to have a similar effect as humic substances on the AD process.

Hydrolysis is the degradation of complex polymeric substrates by the action of enzymes which are proteinaceous molecules that catalyse biochemical reactions. The mechanism of catalytic hydrolysis is defined by the “lock-and-key model” or the “induced-fit model”. Hydrolysis of cellulose and proteins is carried out by various cellulases and proteases and the process are affected by various environmental factors such as temperature and pH, generally applied in AD. Also, various studies suggest that HAs and FAs inhibit hydrolysis which can be mitigated to some extent by the addition of multi-valent metals or excess enzymes. Furthermore, models such as first-order kinetics, Michaelis-Menten kinetics, surface-based kinetics are used to describe the rate of hydrolysis depending on the type of substrate and enzyme activity used in the study. The rate of hydrolysis of soluble substrate is often well defined by Michalis-Menten kinetics.

This review was aimed at achieving an up to date overview and better understanding of the hydrolysis of cellulose and proteins and the known effects of HAs and FAs on hydrolysis in AD. This study will further be conducted to access the impact of melanoidins and metals on the rate of hydrolysis. For this purpose, cellobiose and casein will be used as a substrate and β-glucosidases and Protease as hydrolysing enzymes respectively.

3

Experimental procedures

3.1 Characteristics of Melanoidins

The melanoidins used in the study were prepared by mixing 0.25 M glycine, 0.25 M glucose, and 0.125 M sodium carbonate and autoclaving for 3 hr at 121° C (Migo et al., 1993). The melanoidins were stored below 4°C. The melanoidins were then characterised by testing pH, Chemical Oxygen Demand (COD), Total Organic Carbon (TOC), Total Suspended Solids (TSS), and Volatile Suspended Solids (VSS).

COD and TOC were tested using the Hach Lange LCK014 of range 1,000 – 10,000 mg/L O_2 (Hach Company, USA) and Hach Lange LCK380 (difference method) of range 2 – 65 mg/L C (Hach Company, USA) respectively. TSS and VSS of the melanoidins were tested using Standard Methods described in APHA, 1992. UV absorbance was recorded at 254nm, in a 1 cm path length quartz cell using a spectrophotometer. The colour intensity was recorded at a wavelength of 475 nm in a 1cm path length acryl cell and converted to Pt-Co units using a calibration curve prepared with a standard solution of concentration 500 mg Pt-Co/L.

Size Exclusion Chromatography- High performance liquid chromatography (SEC-HPLC) was performed with ultrafast liquid chromatography (UFLC) system - Prominence LC-20AD XR (Shimadzu, Japan) for molecular size fractionation of melanoidins. The column used was Yarra™ 3 µm SEC-2000, LC Column 300 × 7.8 mm, Ea (Phenomenex, USA). Polystyrene sulfonate standards (Polymer standard service, Germany) were used for the calibration in specific MWs. The method used was adopted with some variations from a protocol developed by Asakawa et al. (2011) and Zahmatkesh et al. (2017) for molecular size fractionation of Humic acids. The details of the method are provided in Table 1 below.

Table 1: Instrument Operating conditions for SEC-HPLC

SEC-HPLC Parameters	
Column	Yarra™ SEC-2000, LC Column 300 × 7.8 mm, 3 µm particle size
Mobile phase	0.01 M Sodium phosphate buffer (pH 7): Acetonitrile 3:1, v/v
Flow	1 mL/min
Volume Injected	25 µL
UV Detection	254 nm and 210 nm
Total Time of elution	15 min

3.2 Determining Melanoidins and Metals interaction

3.2.1 Ultra-filtration coupled with ICP-MS

A test using Ultra-filtration and Inductively coupled plasma mass spectrometry (ICP-MS) was conducted to determine the interaction of melanoidins with metals Na^+, Mg^{2+} Ca^{2+}, Cu^{2+}, $Fe^{2+,}$ and compound NH_4^+. Each cation was tested individually to understand its extent of interaction with

melanoidins. The maximum concentration of melanoidins used was 20 mM which in terms of TOC (2.04 g/L) is representative of the concentration normally found in AD using THP for sludge pre-treatment (Dwyer et al., 2008). The concentration of metals tested was 1mM, 2mM, and 3mM.

Cations addition was done using salts NaCl, NH_4Cl, $MgCl_2$, $CaCl_2$, $FeCl_2$ and $CuCl_2$. 50 mL solution of melanoidins and cations for ultra-filtration were prepared with ultra-pure water as shown in Table 2.

Table 2: Experimental runs for Ultra-filtration coupled with ICP-MS test

Run	Factor 1 A: Melanoidins (mM)	Factor 2 B: Cation (mM)
1	0	1
2	0	2
3	0	3
4	10	1
5	10	2
6	10	3
7	20	1
8	20	2
9	20	3

Batch ultra-filtration was carried out at room temperature using the Ultra-filtration unit Amicon™ Stirred Cells (Merck Millipore, USA) with 1 kDa Ultracel® regenerated cellulose membrane (Merck Millipore, USA) at a pressure of 3 bar using argon as shown in Figure 5. A 5 mL sample of the permeate was collected.

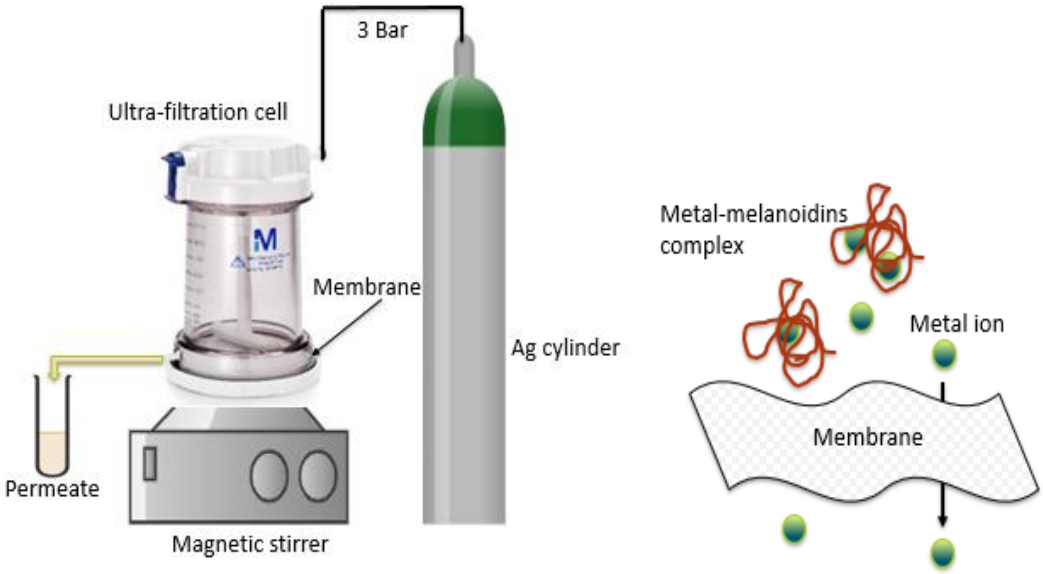

Figure 5: Schematic diagram of the experimental set-up

Samples from the solution and the permeate after ultra-filtration were acidified with HNO_3 - 1% (v/v) to dissolve all solids before testing the concentration of metals by ICP-MS - PlasmaQuant MS (Analytik

Jena, Germany). The ICP-MS analysis for Ca^{2+}, Fe^{2+}, and Cu^{2+} was performed in triplicates. The instrumental operation conditions are given in Table 3. The concentration of compound NH_4 was measured using Hach Lange LCK304 (Hach Company, USA). The percentage of ions in the permeate was calculated by Eq. 2.

$$\%\ of\ ions\ in\ the\ permeate = \frac{Cp}{Cs} * 100 \qquad \text{Eq.2}$$

with:

Cs - concentration of ions in solution before ultra-filtration (mg/L)

Cp - concentration of ions in permeate (mg/L)

Table 3: Instrument Operating conditions for ICP-MS

ICP-MS Parameters	
Forward power	1400 W
Plasma cooling gas	9 L/min (Ar)
Plasma auxiliary gas	1.35 L/min (Ar)
Nebulizer gas flow	1.07 L/min. (Ar)
Peristaltic pump	12 rpm
Sample Uptake flow	5 sec
Resolution	High - ^{23}Na, ^{44}Ca, ^{23}Mg Medium - ^{56}Fe, ^{65}Cu
Mass analyser	Quadrupole
Internal standard	Sc45 / Y89 / In115 / Tb159 (Analytik Jena)
Metals monitored	^{23}Na, ^{39}K, ^{44}Ca, ^{23}Mg, ^{56}Fe and ^{65}Cu

3.2.2 SEC - HPLC coupled with ICP-MS

To understand the variation in the interaction between melanoidins and Ca^{2+}, Cu^{2+} and Fe^{2+} metals with a change in MW of melanoidins, a test was conducted using SEC-HPLC in combination with ICP-MS (Junias et al., 2018). The test was performed for 5 mM and 10 mM melanoidins and 2 mM of each metal as given in Table 4. SEC-HPLC was performed to detect an increase in MW of melanoidins due to interaction with Ca^{2+}, Fe^{3+}, and Cu^{2+} by absorption at 254 nm. The instrument operating conditions, and details of the method are provided in Table 1.

Table 4: SEC-HPLC - ICP-MS Experiments

Run	Metal	Melanoidins (mM)	Metal (mM)
1	-	5	-
2		10	-
3	Ca^{2+}	5	2
4		10	2
5	Fe^{3+}	5	2
6		10	2
7	Cu^{2+}	5	2
8		10	2

The eluent after detection was collected by a sample collector in 3 parts – before elution of melanoidins (0 – 4 min), with melanoidins (4 – 11 min), and after elution of all melanoidins (11 – 15 min) as shown in Figure 6. The collected sample was then tested for the concentration of metals by ICP-MS in order to check if the concentration of metals was higher in the sample with melanoidins than the sample without the melanoidins, which would then confirm the interaction of metals with melanoidins. The mass balance of metals collected by the sample collector was performed. The theoretical mass of metals was calculated from the initial concentration of metal in the sample (2mM) and the volume injected (25µL) in the SEC-HPLC column.

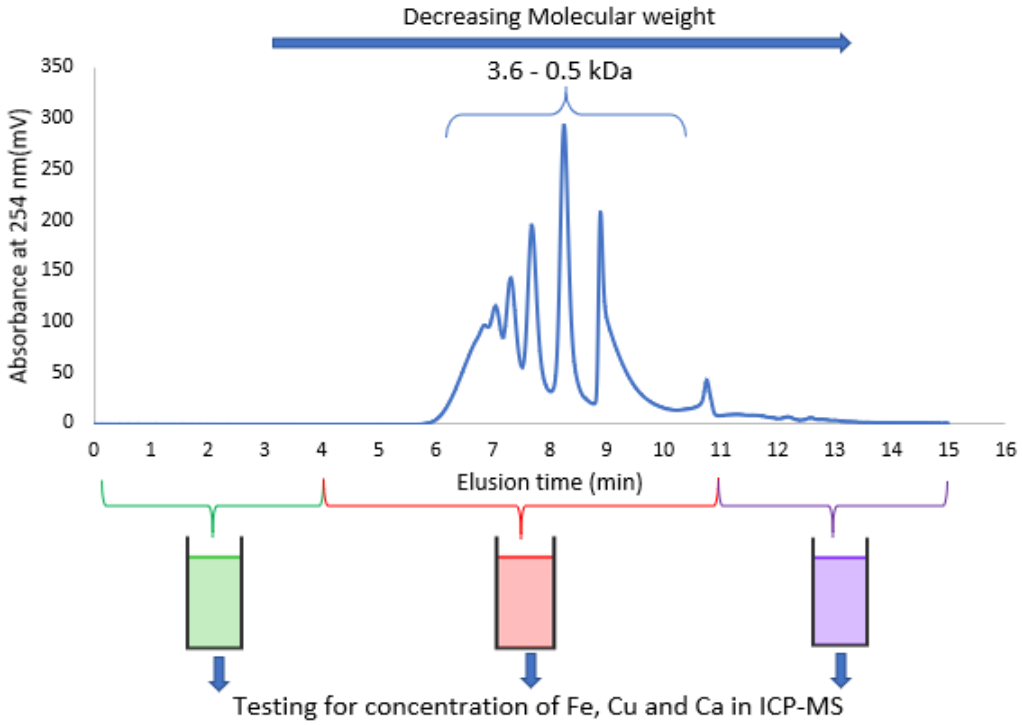

Figure 6: Melanoidins-Metal interaction test with a combination of SEC-HPLC & ICP-MS

3.3 Determining the Rate of Hydrolysis

Cellulase and Protease activity was measured using a Fluorescent Cellulase Assay kit (Marker Gene Technologies Inc., USA) and Pierce Fluorescent Protease Assay Kit (Thermo Fisher Scientific, USA) respectively. The enzymes used were Cellulase from Trichoderma Reesei (CAS No. 9012-54-8, activities ≥ 700 U/g, Sigma-Aldrich, USA) and Protease from *Bacillus sp.* (activities ≥ 16 U/g, Sigma-Aldrich, USA).

The activity of cellulase was determined by reading the increase in fluorescence caused by the release of product Resorufin upon cleavage of fluorescent cellulose substrate, Resorufin Cellobioside used in the assay. The florescence was measured using Synergy™ HTX Multi-Mode Microplate Reader (BioTek, Vermont, USA). Fluorescence was monitored using the Instrument operational conditions given in Table 5. The instrument was used in combination with Gen5 Software for data collection, analysis, exporting, and reporting.

Similarly, the protein substrate - FTC-Casein was digested into smaller fluorescein-labelled fragments by the protease increasing the total fluorescence thus measuring the activity of protease used. The florescence was measured using FLUOstar Galaxy Multi-functional Microplate Reader (BMG

technologies, UK) with the instrument operational conditions as given in Table 5. The enzyme activity assay was performed in Corning® 96-well Black Flat Bottom Polystyrene Not Treated Microplate (Corning Inc., USA) for both the test.

Table 5: Instrument Operating conditions for Microplate Reader

Microplate reader Parameters		
	For Cellulase	**For Protease**
Micro-plate reader	Synergy™ HTX Multi-Mode Microplate Reader	FLUOstar Galaxy Multi-functional Microplate Reader
Detection mode	Fluorescence	
Read Method	End point - Florescence measured one time at the end of the complete reaction (for calibration curve) Kinetics - Florescence measured at regular intervals until the end of the complete reaction (for kinetics of hydrolysis)	
Microplate used	Corning® 96-well Black Flat Bottom	
Temperature	35°C	
Light source	Tungsten halogen	High energy Xenon flash lamp
Detector	Photomultiplier tube	
Shaking	Orbital shake (10 sec between each read in kinetics)	Orbital shake (5 sec at 140 rpm between each read in kinetics)
Reading Interval for Kinetics	1 min for 45 min	1.67 min for 60 min
Suggested Ex/Em Wavelength in the kit	571/585 nm	485/538 nm
Used Ex/Em Wavelength for the test	530 ± 25/590 ± 35	485/520 nm

A 3-Level factorial design with three independent variables (A: melanoidins, B: Iron, C: Copper) was performed by applying the Design Expert 12 software, in order to prepare data for statistical calculation. The maximum concentration of melanoidins and metal used for the test was 10 mM (TOC=1.02 g/L) and 3 mM respectively. The design had 6 times central point replications which lead to 32 experimental runs as shown in Table 6.

The concentration of Resorufin Cellobioside and FTC-Casein used to perform the test was 0.025 mM and 0.05 mg/mL respectively. For every experimental run, a Blank - without substrate and enzyme was measured to account for the auto fluorescence/absorbance due to presence of melanoidins and metal. The calibration curve was prepared separately for each experimental run to compensate for the interference in fluorescence measurement by the presence of a different concentration of melanoidins and metals. The calibration curves for Cellulase activity were determined using Resorufin standard in concentrations of 0.025 mM, 0.0125 mM, and 0.0005 mM and had an average R^2 value greater than 0.986. Whereas calibration curves for protease assay were prepared by measuring the endpoint fluorescence after hydrolysis of 0.005 mg/mL, 0.00125 mg/mL and 0.000625 mg/mL FTC-Casein and enzyme TPCK-Trypsin provided in the kit.

The effect of different concentrations of melanoidins, Fe^{3+}, Cu^{2+} on hydrolysis was studied by calculating the maximum rate of hydrolysis (V_{max}) using a MATLAB code which correlates the fluorescence (RFU) and product concentration considering the calibration curve prepared for each run.

The MATLAB code used has been given in Annexure 1. V_{max} was used to solve for Michaelis-Menten model for hydrolysis as presented by equation 3.

$$\frac{dP}{dt} = \frac{V_{max}(S_0 - P)}{K_s + (S_0 - P)} \quad \text{Eq.3}$$

where,

V_{max} = maximum rate of hydrolysis (mmoles/L*min)

S_0 = Initial concentration of substrate (mmoles/L)

P = product concentration at time t (mmoles/L)

K_s = substrate affinity (mmoles/L)

The V_{max} calculated was then added as a Response to the 3-Level factorial design to find the best Response Surface Model (RSM) to fit the data. Analysis of Variance (ANOVA) test was applied to evaluate the adequacy (by applying the lack-of-fit test) of different models and to evaluate the statistical significance of the factors in the model. In order to examine the goodness and evaluate the adequacy of the fitted model, the coefficient of determination R^2 was calculated. Design Expert 12 software was employed for the regression analysis and graphical optimization.

Table 6: 3-Level Factorial Design matrix for Hydrolysis Experiment

Run	Factor 1 A: Melanoidins (mM)	Factor 2 B: Iron (mM)	Factor 1 C: Copper (mM)
1	10	1.5	1.5
2	5	1.5	1.5
3	5	3	1.5
4	0	3	1.5
5	5	1.5	3
6	10	1.5	3
7	0	0	3
8	10	0	3
9	10	0	0
10	0	3	0
11	5	1.5	1.5
12	0	3	3
13	5	3	3
14	5	0	3
15	5	1.5	0
16	5	0	1.5
17	10	3	1.5
18	0	1.5	0
19	10	0	1.5
20	5	1.5	1.5
21	0	0	1.5

Run	Factor 1 A: Melanoidins (mM)	Factor 2 B: Iron (mM)	Factor 1 C: Copper (mM)
22	0	1.5	1.5
23	5	1.5	1.5
24	5	1.5	1.5
25	0	0	0
26	5	1.5	1.5
27	10	1.5	0
28	10	3	3
29	0	1.5	3
30	10	3	0
31	5	0	0
32	5	3	0

3.4 Determining the mechanism in which melanoidins interfere

SEC-HPLC was used to determine the mechanism which might play a role in the increase/ decrease of the rate of hydrolysis in the co-presence of melanoidins and metals. Two major hypotheses as presented were tested.

Test-1 was performed to check the hypothesis: the carboxylic and phenolic functional groups of melanoidins bind to the active enzymatic sites thus preventing substrate hydrolysis. But, in the presence of metals, metals complex with the carboxylic and phenolic functional groups of melanoidins thus not affecting the active sites of enzymes. Test-2 was performed to check the hypothesis: Cu^{2+} interacts with the enzymes to deactivate the enzymes, while Fe^{3+} facilitates the enzyme-substrate interaction to promote hydrolysis.

The solutions were prepared as presented in Table 7. SEC-HPLC was then performed in triplicates with instrument operating conditions provided in Table 1.

Table 7: Tests performed with SEC-HPLC to determine the mechanism of hydrolysis

Test 1			
Enzyme (U/g)	Melanoidins (mM)	Fe^{3+} (mM)	Cu^{2+} (mM)
0.7	-	-	-
-	5	-	-
0.7	5	-	-
0.7	5	2	-
0.7	5	-	2

Test 2				
Enzyme (U/g)	Substrate (mM)	Melanoidins (mM)	Fe^{3+} (mM)	Cu^{2+} (mM)
-	0.025	-	-	-
0.7	0.025	-	2	-
0.7	0.025	-	-	2
0.7	0.025	5	2	-
0.7	0.025	5	-	2

4

Results and Discussion

4.1 Characteristics of Melanoidins

The characteristics of the melanoidins used in the study are presented in Table 8. The TOC of the melanoidins was 25.5 ± 1.5 g/L, while the COD was 68.8 ± 4.6 g/L. The TS and VS of the melanoidins were 55.6 ± 0.1 g/L and 32.0 ± 0.9 g/L respectively. Colour of 251.5 x 10^3 ± 1913.0 mg Pt-Co/L was recorded at 475 nm and an absorbance of 604.0 ± 0 cm^{-1} at 254 nm. In all the procedures the pH of melanoidins used was 6.00 ± 0.05. The melanoidins used to study hydrolysis in this work were of maximum concentration of 10mM which in terms of TOC and COD are 1.02 g/L and 2.75 g/L respectively.

Table 8: Characteristics of Melanoidins

Characteristics of Melanoidins	
pH	6.00 ± 0.05
TOC	25.5 ± 1.5 mg/L
COD	68.8 ± 4.6 mg/L
TS	55.6 ± 0.1 g/L
VS	32.0 ± 0.9 g/L
Colorimetry 475 nm	251596.7 ± 1913.0 mg Pt-Co/L
UV254	604.0 ± 0 cm^{-1}

Figure 7 presents the SEC chromatogram of 5 mM melanoidins at 254nm and 210nm. The percentage of melanoidins with MW between 3.6 - 1.1 kDa was 28%, between 1.1- 0.5 kDa was 71% and only 1 % have MW < 0.5 kDa. The UV absorbance ratio (UVA_{210}/UVA_{254}) was calculated at each peak and shown in Figure 7. The ratio ranges from 1.56 to 1.75 which is similar to the ratios found commonly in HAs (1.59, highest aromaticity) and FAs (1.88, intermediate aromaticity) (Her et al., 2008). The relatively higher UVA_{210}/UVA_{254} ratio of 1.72 and 1.75 in the MW range 1.1- 0.5 kDa suggest the higher density of functional groups (OH and COOH) while relatively lower UVA_{210}/UVA_{254} ratio of 1.56 in MW range of 3.6- 1.1 kDa signifies higher density of aromatic rings (Her et al., 2008).

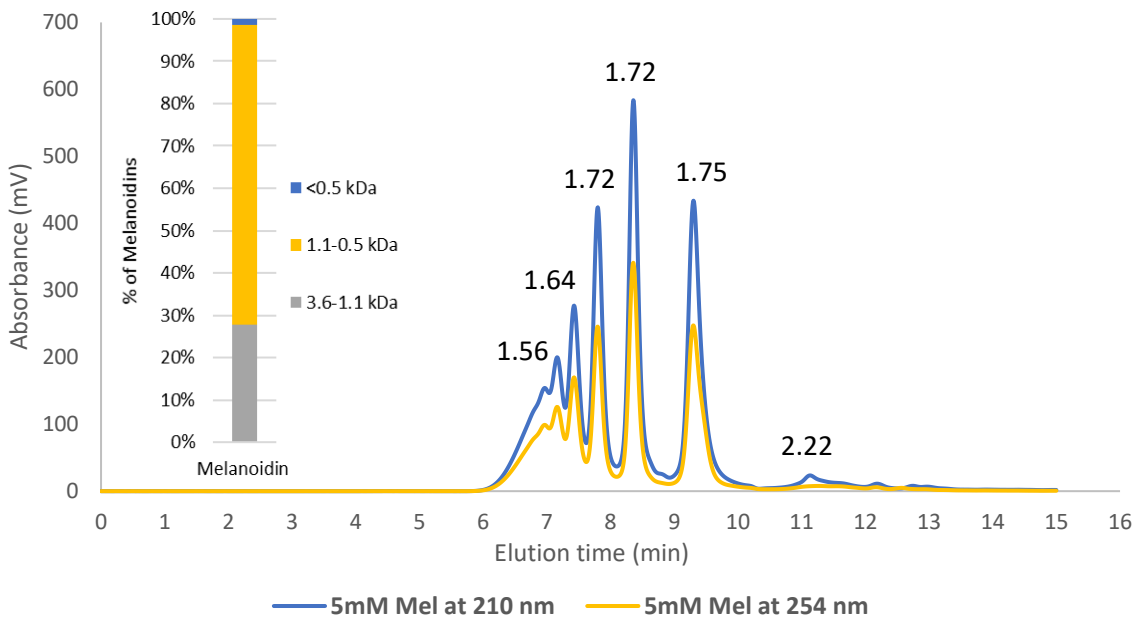

Figure 7: SEC chromatogram of 5 mM Melanoidins at 254 nm with % molecular weight distribution

4.2 Melanoidins and Metals interaction

4.2.1 Ultra-filtration coupled with ICP-MS

The ability of metals to complex with the melanoidins is shown in Figure 8 by the percentage of ions concentration in the permeate after ultra-filtration compared with the total initial concentration of ions. In the absence of melanoidins, 95 % of Cu^{2+} and Mg^{2+} ions pass through the membrane. The percentage of ions that pass through the membrane in the case of NH_4^+, K^+, Ca^{2+}, and Fe^{2+} increases with an increase in ion concentration from 1 mM to 3 mM due to an increase in ionic strength as seen in Figure 8(a).

It is evident from Figure 8(b) and Figure 8(c) that the concentration of ions passing through the membrane in the presence of melanoidins decreases owing to the ions-melanoidins interaction. The ability of HAs to bind to cationic metals to form complexes has been studied for its applications in the removal of heavy metals from soil and water (Yates & Von Wandruszka, 1999). As per the studies of von Wandruszka (2000), the interaction between HA molecules and metal cations was initially entirely electrostatic, and the cations moved to their thermodynamically preferred locations within the structure forming spherical HA-metal complexes. This interaction varies with different metals and was influenced by the metal concentration, origin and MW, and concentration of HA.

From Figure 8, Fe^{2+} ions passing through the membrane decreases to 30 % and 28 % with 1 mM ions and 10 mM and 20 mM melanoidins respectively due to the formation of melanoidins-metals complexes. Fe^{2+} shows higher interaction than the other di-valent ions (Ca^{2+}, Mg^{2+},and Cu^{2+}) maybe because of air oxidation of some Fe^{2+} ions to Fe^{3+} ions in water (Ahcllar et al., 2016). Then the interaction of tri-valent ions with the negatively charged phenolic and carboxyl groups of melanoidins is stronger than that of di-valent cations (Alpatova et al., 2004; Gomyo & Horikoshi, 1976).

The percentage of ions concentration in the permeate of 1 mM Ca^{2+}, Mg^{2+} and Cu^{2+} with 10 mM melanoidins is 62 %, 59 % and 50 % respectively as seen in Figure 8(b). A similar trend is shown with 2 mM and 3 mM metal concentrations. This suggest that melanoidins-metals complexation for Ca^{2+} >

Mg^{2+} > Cu^{2+} due to the difference in the ionic size of these metals. Amongst the metal ions with a similar charge, the ion with higher ionic radius was able to interact with the organic compounds more effectively, particularly HAs (Alpatova et al., 2004). For the metals tested, the ionic radius of Ca^{2+} > Mg^{2+} > Cu^{2+} (Slater, 1965). The 98% pass-through of Ca^{2+} ions obtained for 1 mM Ca^{2+} and 20 mM melanoidins can be regarded as an outlier.

On average, 80 % of the total K^{+} ions concentration passes through the membrane at all initial metal and melanoidins concentration as seen in Figure 8. The ability of melanoidins to bind polyvalent cations is higher than mono-valent cations. The oxygen containing functional groups such as carboxylic, phenolic, carbonyl attribute to the high binding of polyvalent ions to HAs (Alpatova et al., 2004). The ability of NH_4^{+} to bind with the melanoidins is negligible considering that on an average 90 % of the ions pass through the membrane in presence of 10 mM and 20 mM melanoidins.

As observed from Figure 8, the percentage of di-valent cation concentration in the permeate was lower with 20 mM melanoidins than 10 mM at a constant metal concentration. This means the melanoidins-metal interaction increased with an increase in melanoidins concentration as there were more phenolic and carboxylic functional groups available for binding. Kim et al. (2005) made similar observations while studying the removal of Co^{2+} with HAs as complexing agents to enhance membrane separation.

Moreover, for constant melanoidins concentration, the melanoidins-metal interaction decreased with an increase in di-valent metal concentration from 1 mM to 2 mM. This is assumed to be due to the increase in the ionic strength of the solution. Kim et al. (2005) observed that increasing the ionic strength of initial solution by addition of electrolytes such as NaCl, reduced the complexation of Co^{2+} ion with functional groups of HAs and thus reduced the efficiency of Co^{2+} removal. However, the difference in the melanoidins-metal binding between 2mM and 3mM initial concentration is less. This could be attributed to the saturation of available binding sites in melanoidins. Hankins et al. (2006) studied the removal of Zn^{2+} and Pb^{2+} by addition of HAs and ploy-electrolyte and concluded that for a given HA concentration, there is a little change in metal ion removal as the HA–metal ratio (mass to mass) varies above 2 as an excess of binding sites are already available.

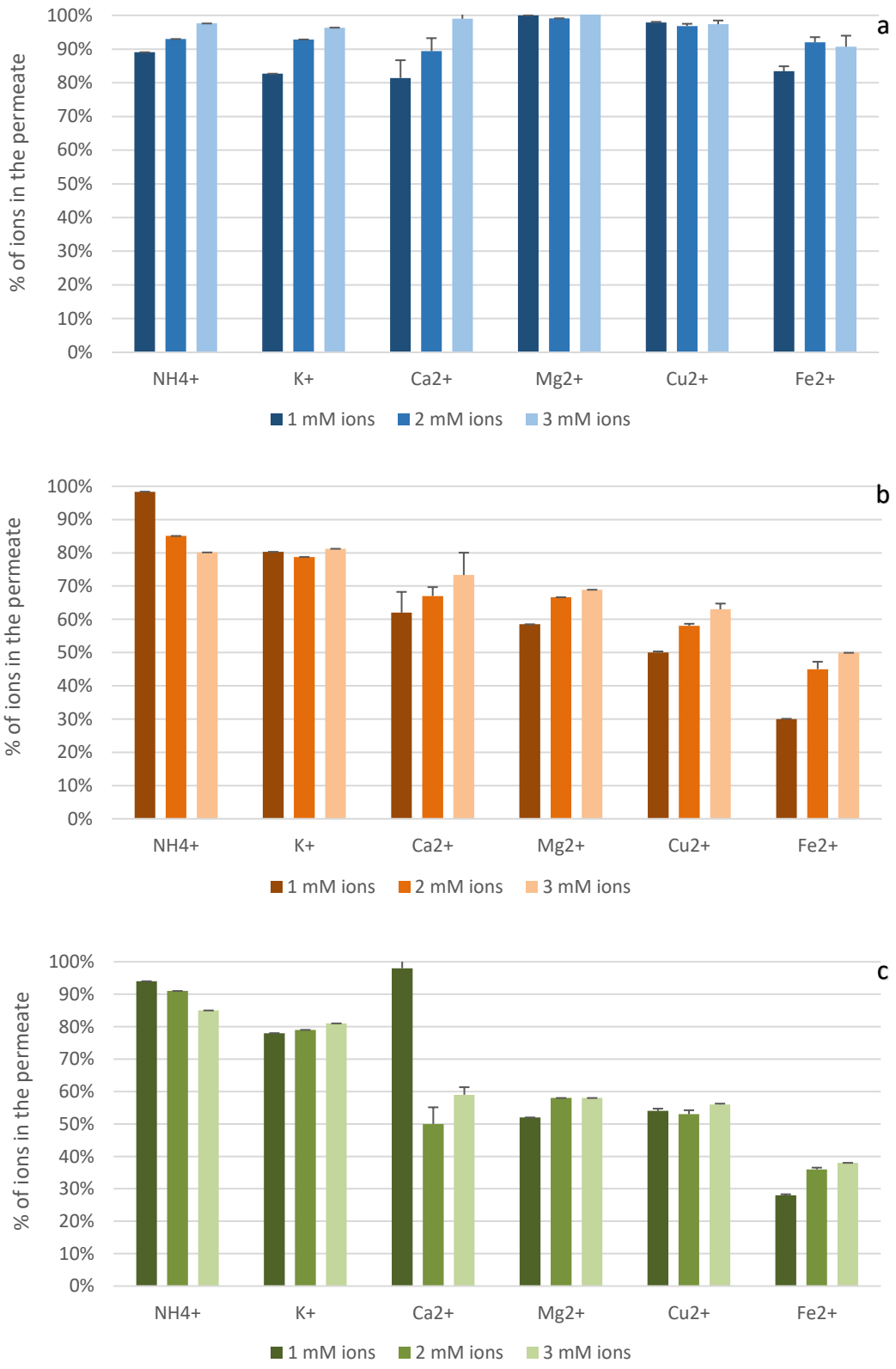

Figure 8: Melanoidins-metal complexation at (a) 0 mM melanoidins, (b) 10 mM melanoidins and (c) 20 mM melanoidins with initial ions concentrations of 1mM, 2mM and 3mM presented as the percentage of ions concentration in permeate compared to initial ion concentration. Bars indicate standard errors (n = 3)

Figure 9 shows the percentage of melanoidins concentration in the permeate after ultra-filtration in comparison to initial melanoidins concentration measured using absorbance at 475nm. The results show that approximately 80 % of melanoidins are larger than 1kDa. The concentration of melanoidins in the permeate for mono-valent cations is on an average 5 % higher than for di-valent cations however, no other trends are seen that relate to melanoidins-metals complexation. Therefore, the interactions of metals with melanoidins do not affect the retention of melanoidins by UF (Alpatova et al., 2004)

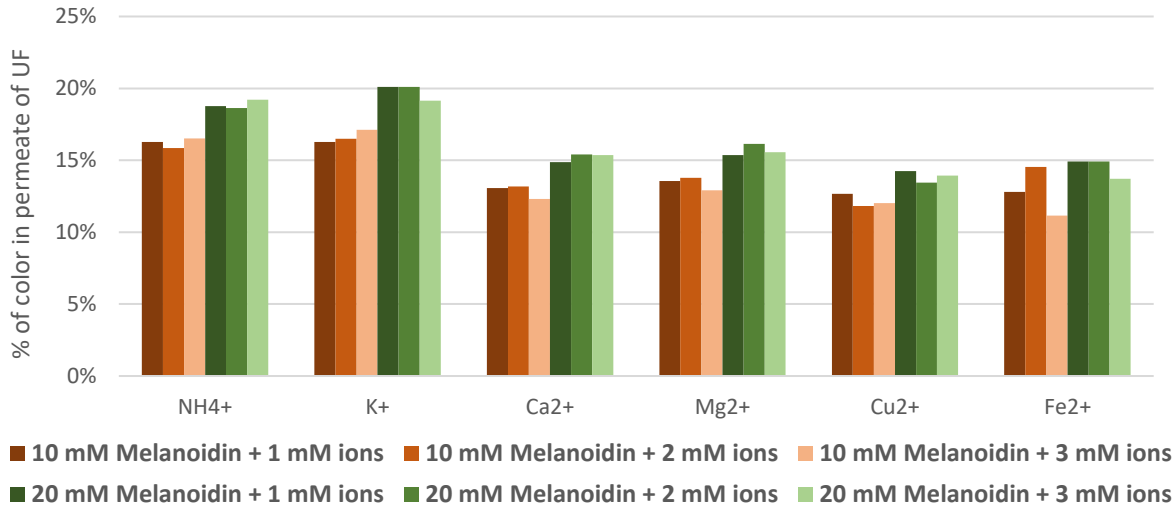

Figure 9: Percentage of Melanoidins concentration in the permeate after Ultra-filtration compared to initial melanoidins concentration measured using absorbance at 475nm

4.2.2 SEC-HPLC

Figure 10(a) shows the SEC-HPLC chromatogram of melanoidins in the presence of Fe^{3+}, Cu^{2+}, and Ca^{2+} for absorbance at 254nm. It is noteworthy that the MW decreases with an increase in elution time. To facilitate the comparison of SEC results, each SEC chromatogram was divided into five regions based on major detected peaks, and the area below the peak was presented as stacked columns, as shown in Figure 10(b).

Figure 10(a) shows that the melanoidins elude earlier in the presence of Fe^{3+} showing an increase in MW caused by melanoidins-metal complexation, while no major change in observed in the presence of Cu^{2+} and Ca^{2+}. It is observed that in presence of 2mM Fe^{3+} and 5mM melanoidins, the area below the graph in the size range 29 - 3.6 kDa and 3.6 - 1.1 kDa increases from 2 to 140 and from 99 to 126. While the area below the graph in the size range 1.1 - 0.5 kDa decreases from 221 to 192. This suggests an increase in MW of melanoidins due to Fe^{3+} complexation with smaller MW melanoidins. A similar pattern is observed in MW distribution with 10mM melanoidins concentration from Figure 10(b).

Christl & Kretzschmar (2001) studied the relation between the MW of HAs and FAs and the amount of carboxyl carbon and phenolic carbon using carbon content and ^{13}C NMR spectra. The carboxylic and phenolic carbon increased with decreasing average molecular weight in HAs. Also, the FAs contained more carboxylic and slightly more phenolic carbon than HAs. The FAs exhibited much higher negative charge than HAs at a given pH and during potentiometric titration, the negative charge of FAs decreases faster than of HAs meaning phenolic and carboxylic groups functional groups contribute most to the proton and metal cation binding behaviour of HAs and FAs.

Therefore, the melanoidins of smaller MW (1.1 – 0.5 kDa) which have a higher density of hydroxyl and carboxyl groups as presented in section 4 facilitate the binding of melanoidins with di-valent and tri-valent cations. Though the difference in the amounts of phenolic and carboxyl groups might be small due to smaller variations in the MW distribution of the melanoidins used in the study.

As seen from Figure 10, no change in MW of melanoidins is observed with Cu^{2+} and Ca^{2+} ions, but the results obtained from ultra-filtration coupled with ICP-MS shows complexation with these ions. Fe^{3+} has higher binding capacity to the negatively charged carboxyl and phenolic groups of melanoidins which leads to charge neutralisation and thus inter-molecular complexation which increases the MW of melanoidins. This increase in MW is detected well in the SEC-HPLC. Whereas, Cu^{2+} and Ca^{2+} although could interact with melanoidins to some extent cannot lead to high charge neutralisation and thus the residual negative charge on melanoidins prevent a transition from intra-molecular complexes to inter-molecular ones. Therefore, the change is MW which is not as high as in the case of Fe^{3+} cannot be detected in SEC-HPLC. This might be like the effect Fe^{3+} has on HAs removal at different pH. At lower pH, the HAs are removed due to charge neutralisation and flocculation while at higher pH the formation negatively charged flocs of $Fe(OH)_3$ due of hydrolysis of Fe limit charge neutralisation and coagulation decreasing the efficiency of HAs removal (Cheng, 2002).

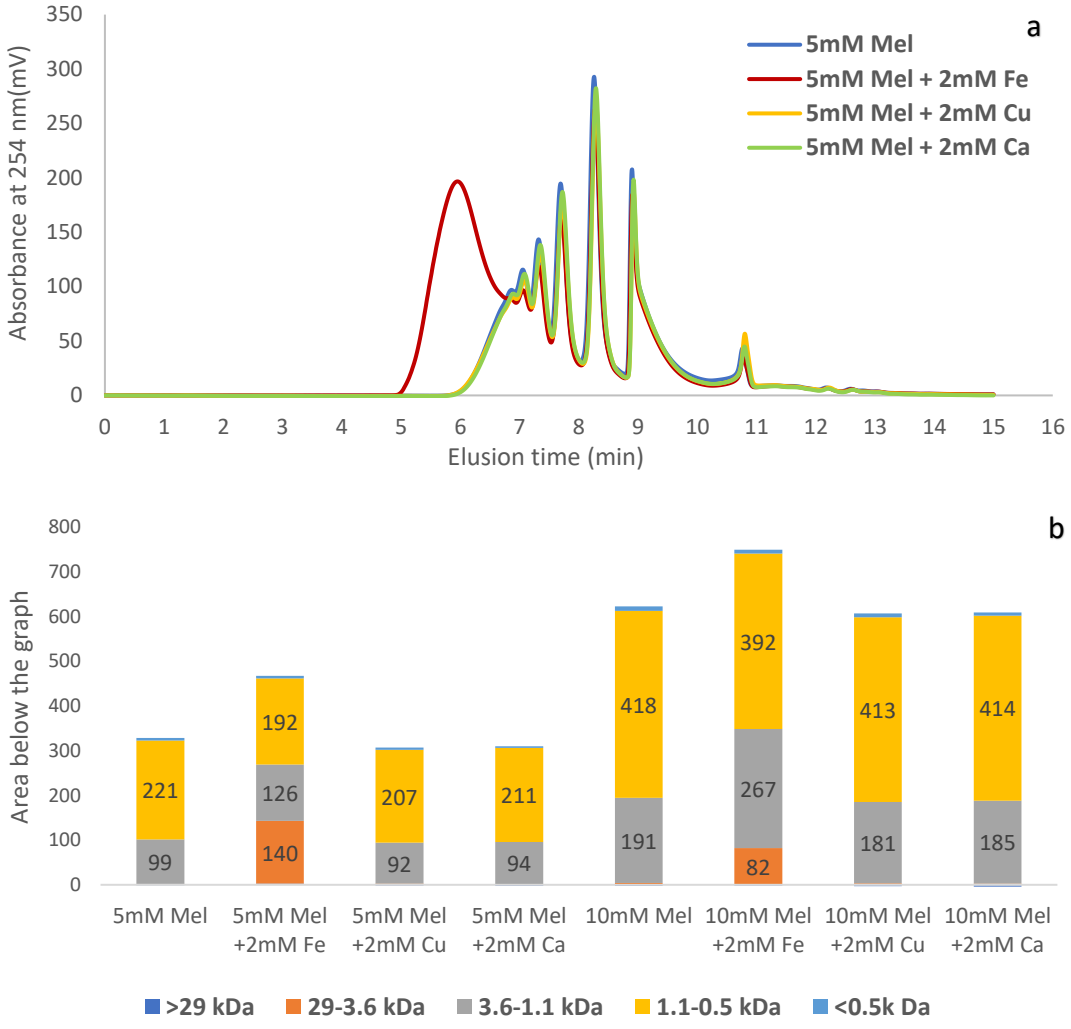

Figure 10: SEC-HPLC of 5mM and 10mM melanoidins with 2mM Fe^{3+}, Cu^{2+} and Ca^{2+} each (a) SEC-HPLC chromatogram and (b) % molecular weight distribution of melanoidins

4.2.3 SEC-HPLC coupled with ICP-MS

The samples of the eluent from SEC-HPLC were collected by sample collector in 3 parts - before elution of melanoidins (1 - 4 min), with elution of melanoidins (4 - 11 min) and after elution of all melanoidins (11 - 14 min). Figure 11(a) shows the mass balance of metals in the eluent and Figure 11(b) represents the distribution of the concentration of metals in 3 collected parts. The mass of unaccounted ions was calculated by subtracting the mass of metals collected in the eluent of SEC-HPLC from the calculated theoretical mass of metals injected in the system.

The unaccounted ions in the case of Fe^{3+} were 45 % while that for Cu^{2+} were 90 %. The mass of ions that are not collected in the eluent could be due to loss of mass in the part of eluent that was not collected in the method or due to chloride interference with the SEC-HPLC column.

The concentration of Fe^{3+} in the eluent collected between 4 - 11 min was 0.23 mg/L and 0.19 mg/L for 5mM and 10mM melanoidins respectively. This concentration is much higher than 0.01 mg/L Fe^{3+} in the eluent collected between 1 - 4 min and 11 - 14 min in both the cases. The higher concentration of Fe^{3+} with melanoidins proves the formation of melanoidins-Fe complexes in the system.

The concentration of Cu^{2+} ions in the time range 11 - 14 min was 0.02 mg/L and 0.04 mg/L for 5mM and 10mM melanoidins. This concentration is almost similar to 0.02 mg/L concentration of Cu^{2+} in the samples without melanoidins. However, almost 90 % of the Cu^{2+} metals were lost in the system and could have eluted in any of the 3 different time phases making a huge difference in the results then obtained. Therefore, the results obtained for Cu^{2+} concentrations cannot be considered reliable with 90 % of the Cu^{2+} mass is unaccounted.

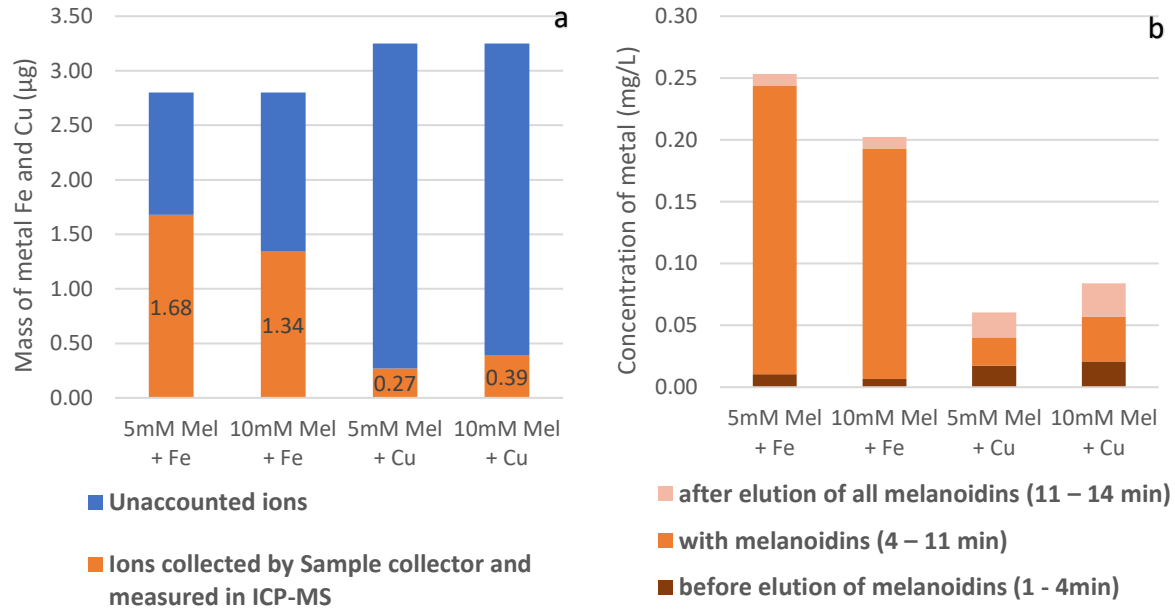

Figure 11: SEC-HPLC - ICP-MS results with 5mM & 10mM melanoidins and 2mM Fe^{3+}, Cu^{2+} (a) mass balance of metals collected by sample collector in SEC-HPLC, (b) concentration of metals measured by ICP-MS for samples collected before, with and after elution of melanonids in SEC-HPLC

4.3 Rate of Hydrolysis

4.3.1 Cellulose hydrolysis

4.3.1.1 Preliminary test with metals Ca^{2+}, Fe^{3+}, and Cu^{2+}

The effect of different concentrations of melanoidins, Fe^{3+}, Cu^{2+} and, Ca^{2+} on hydrolysis of cellulose was studied by calculating the maximum rate of hydrolysis (V_{max}) for all the 87 experimental runs as per a three-level factorial design presented in Annexure 2. The F-value tests were performed using ANOVA to calculate the significance of individual parameters (A: melanoidins, B: Ca^{2+} C: Fe^{3+} and D: Cu^{2+}) and there interaction terms (AB, AC, AD, BC, BD, and CD) for a 2FI model as presented in Table 9. The p-values of terms B: Ca^{2+}, AB, BC, and BD were 0.1827, 0.2687, 0.6463, and 0.7143 respectively, which implied that Ca^{2+} concentration had no significant impact on the response (V_{max}). All the other parameters – melanoidins, Fe^{3+}, and Cu^{2+} had a significant impact on V_{max} and were further tested and analysed.

Table 9: Preliminary test - Analysis of Variance for 2FI model

Source	F-value	p-value	
Model	8.74	< 0.0001	significant
A-Melanoidin	15.04	0.0002	
B-Calcium	1.81	0.1827	Not Significant
C-Iron	0.3161	0.5756	
D-Copper	29.78	< 0.0001	
AB	1.24	0.2687	Not Significant
AC	7.47	0.0078	
AD	31.28	< 0.0001	
BC	0.2123	0.6463	Not Significant
BD	0.135	0.7143	Not Significant
CD	0.0968	0.7566	Not Significant

4.3.1.2 Test with metals Fe^{3+} and Cu^{2+}

Fluorescence decay was observed with increasing concentration of product Resorufin in the enzymatic assays as shown in Annexure 3. Therefore, a decay factor (K_d) was calculated and the V_{max} was compensated for this decay of fluorescence. The results of the V_{max} obtained for all the 32 experimental runs are presented in Table 10. As seen the results, the V_{max} for blank - without addition of melanoidins and metals was 2.037 µmoles/L * min. The maximum rate of hydrolysis was 2.817 µmoles/L * min which occurred with 0 mM melanonids, 0 mM Cu^{2+} and 3 mM Fe^{3+} , while the minimum rate of hydrolysis was 0.322 µmoles/L * min and occurred with 0 mM melanoidins, 0 mM Fe^{3+} and 3 mM Cu^{2+}.

Table 10: Maximum rate of hydrolysis (V_{max}) for the Michaelis-Menten kinetic model for the 3-level factorial design

Run	**Parameter A:** Melanoidins (mM)	**Parameter B:** Iron (mM)	**Parameter C:** Copper (mM)	**Response 1:** V_{max} (µmoles/L*min)
1	10	1.5	1.5	0.958
2	5	1.5	1.5	1.626
3	5	3	1.5	2.189
4	0	3	1.5	2.541
5	5	1.5	3	1.066
6	10	1.5	3	0.944
7	0	0	3	0.322
8	10	0	3	0.868
9	10	0	0	1.225
10	0	3	0	2.817
11	5	1.5	1.5	1.198
12	0	3	3	2.404
13	5	3	3	3.126
14	5	0	3	0.704
15	5	1.5	0	1.465
16	5	0	1.5	1.046
17	10	3	1.5	1.682
18	0	1.5	0	2.691
19	10	0	1.5	1.204
20	5	1.5	1.5	1.414
21	0	0	1.5	0.606
22	0	1.5	1.5	2.022
23	5	1.5	1.5	1.041
24	5	1.5	1.5	1.422
25	0	0	0	2.037
26	5	1.5	1.5	1.125
27	10	1.5	0	1.106
28	10	3	3	1.620
29	0	1.5	3	0.965
30	10	3	0	1.039
31	5	0	0	1.358
32	5	3	0	2.687

The results before performing the ANOVA, indicated that the rate of hydrolysis had a positive correlation with Fe^{3+} while a negative correlation with Cu^{2+} and melanoidins. The Pearson correlation of V_{max} with melanoidins, Fe^{3+} and Cu^{2+} was found to be -0.342, 0.638 and -0.262 respectively as represented with heatmap in Figure 12 below.

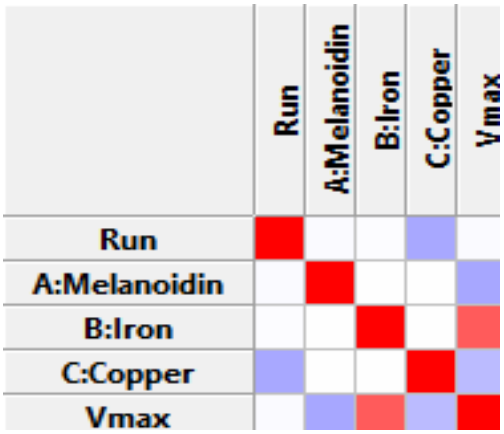

Figure 12: Correlation matrix of V_{max} with melanoidins, Fe^{3+} and Cu^{2+}

The F-value tests were performed using ANOVA to calculate the significance (p-value) of linear, two factor interaction (2FI), quadratic, and cubic type of model. The quadratic and cubic models were not significant ($p > 0.1$) with F-values 2.51 and 1.82 respectively. The 2FI model which was the highest order model with F-value (17.59) and p-value (<0.0001) was chosen. 2FI model is a linear model with the addition of the two-factor interaction (AB, BC, CA) terms (StatEase, 2020).

Besides evaluating the significance, the adequacy of the model was evaluated by applying the lack-of-fit test. This test is used in the numerator in an F-test of the null hypothesis and indicates that a proposed model fits well or not (StatEase, 2020). The test for lack-of-fit compares the variation around the model with pure variation within replicated observations (StatEase, 2020). The lack-of-fit F-value of 2.86 and p-value of 0.1237 for the selected 2FI model implies the lack-of-fit is not-significant and thus the 2FI model is a good fit to the experimental V_{max} values.

After denoting 2FI as the best model with the highest order, the independent variables (A-Melanoidins, B-Iron, C-copper, AB, AC, and BC) were fitted in the specified model and the effect of each variable was evaluated. Table 11 represents the ANOVA of the selected 2FI model. The F-values of independent variables were 15.3, 53.6, 8.97, 9.75, 10.62, and 7.69 respectively, significant with a probability of 99 % or less. This implied that all model parameters have a real and significant effect on the response (V_{max}). Further the R^2 and the adjusted R^2 of the model where 0.89 and 0.76 respectively which illustrated a good correlation between the independent variables and V_{max}.

The regression coefficients which represent the expected change in response V_{max} per unit change in a parameter when all remaining factors are held constant are provided in Table 11. The coefficients for melanoidins, Fe^{3+} and Cu^{2+} are -0.32, 0.60 and -0.25 respectively. This indicates that Fe^{3+} has a large positive impact of V_{max} while melanoidins and Cu^{2+} both decrease the V_{max}. The regression coefficients of the interaction effect of melanoidins+Fe^{3+}, melanoidins+Cu^{2+} and Fe^{3+}+Cu^{2+} are -0.31, 0.33 and 0.28 respectively. This indicates that the inactivation of cellulase due to Cu^{2+} decreases with the addition of melanoidins most likely due to melanoidins-Cu^{2+} complexes. The interaction of melanoidins and Fe^{3+} lowers the V_{max}, but Fe^{3+} individually shows a large positive impact and is more significant to the model. Subsequently, the regression coefficients are used to produce an equation with all 6 independent parameters to make predictions about the response for each of the 32 experimental runs.

Table 11: Analysis of Variance for 2FI model

Source	F-value	p-value		Regression Coefficient
Model	17.59	< 0.0001	Significant	
A-Melanoidins	15.30	0.0006		-0.3199
B-Iron	53.20	< 0.0001		0.5964
C-Copper	8.97	0.0061		-0.2449
AB	9.75	0.0045		-0.3127
AC	10.62	0.0032		0.3264
BC	7.69	0.0103		0.2778
Residual Lack of Fit	2.86	0.1237	Not Significant	
R^2	0.8085			
Adjusted R^2	0.7625			
Predicted R^2	0.6797			

Figure 13 shows that the actual experimentally values of V_{max} are distributed relatively near to the predicted regression line and there is a good correlation between the actual and predicted values. Therefore, the 3-level factorial experimental design can be effectively applied to understand the effect of melanoidins, Fe^{3+}, and Cu^{2+} on the rate of hydrolysis.

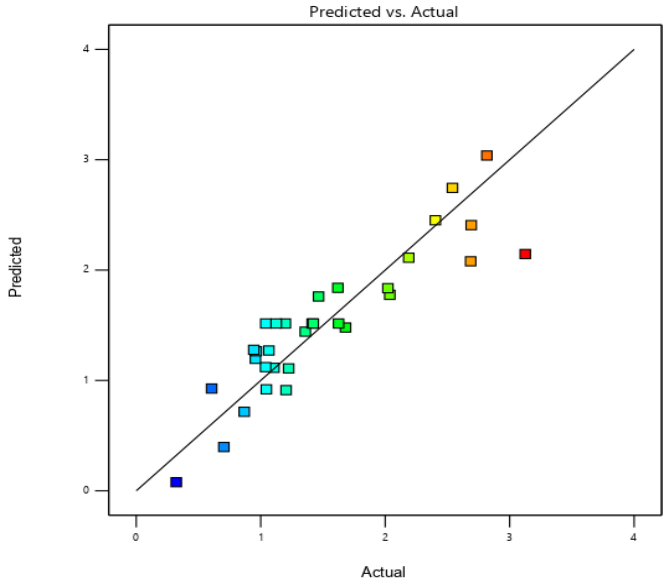

Figure 13: Linear correlation between predicted and actual values of the response

Figure 14 shows the Response surface of the combined effect of Cu^{2+}, Fe^{3+}, and melanoidins on the rate of hydrolysis of cellulose. It was clear from Figure 14(a) (with 0 mM melanoidins) that the rate of hydrolysis was increasing with Fe^{3+} concentration while decreasing with Cu^{2+} concentration. The positive impact of Fe^{3+} could be due to the coagulation effect of Fe^{3+} which facilitates the enzyme-substrate interaction to promote hydrolysis. On the other hand, Cu^{2+} is known to inhibit the activity of enzymes by chemical binding to enzymes leading to subsequent disruption of enzyme structure and function (C. Li & Fang, 2007).

Similar results were found when the activity of cellulase from *Aspergillus niger* was tested with CM-cellulose in the presence of 10mM Cu^{2+}, complete inhibition in enzyme activity was observed (Hurst et al., 1977). Similarly, OKADA (1975) tested the enzymatic activity of cellulase from *Trichoderma viride* and found partial enzyme inhibition in the presence of 1 mM Cu^{2+} while no inhibition with 1 mM Fe^{2+} (OKADA, 1975).

As compared to 0 mM melanoidins, V_{max} at 5 mM melanoidins decreases as seen from Figure 14(b) where the entire plane shifts low. The V_{max} with 0mM metals and melanoidins decreases from 2.04 µmoles/L*min to 1.36 µmoles/L*min with 5 mM melanoidins showing the inhibiting effect of melanoidins on the rate of hydrolysis. The V_{max} with 5mM melanoidins and 3mM Cu^{2+} increases to 0.704 µmoles/L*min from 0.322 µmoles/L*min with 0mM melanoidins and 3mM Cu^{2+}. This could be explained by the formation of melanoidins-Cu^{2+} complexes due to which the concentration of Cu^{2+} available to inhibit the enzyme activity decreases. However, at constant 5mM melanoidins concentration, an increase in Cu^{2+} concentration still inhibits enzyme activity as the melanoidins binding sites are saturated.

The V_{max} in presence of 5mM melanoidins increases from 1.36 µmoles/L*min to 2.68 µmoles/L*min with 0mM Fe^{3+} and 3mM Fe^{3+} respectively. However, as presented in Figure 14(c) at 10mM melanoidins the V_{max} is 1.26 µmoles/L*min in absence of metals while with 3mM Fe^{3+} the V_{max} is decreased to 1.04 µmoles/L*min. This means that at 5 mM melanoidins Fe^{3+} is still freely available to increase the rate of hydrolysis while as the melanoidins concentration increases to 10 mM and more binding sites are available for melanoidins-Fe^{3+} complexation, no more free Fe^{3+} are available for improving the rate of hydrolysis.

It is clear from Figure 14 and Table 11 that melanoidins and Cu^{2+} individually decreases the rate of hydrolysis while Fe^{3+} improves the rate of hydrolysis. As per the results of this study, in the presence of melanoidins, the rate of hydrolysis is improved at higher concentrations of metals Cu^{2+} and Fe^{3+}. It is hypothesised that Cu^{2+} inhibits hydrolysis by inactivating cellulases, but in presence of melanoidins, it facilitates hydrolysis by forming melanoidins-Cu^{2+} complexes thus negating its toxic effect on cellulases. While Fe^{3+} improves hydrolysis by facilitating substrate-enzyme interaction but in presence of melanoidins, melanoidins-Fe^{3+} complexes are formed which reduces the positive impact of Fe^{3+}.

Azman et al. (2015) studied the mitigation of HAs inhibition on anaerobic cellulose digestion with 5 mM of Ca^{2+}, Fe^{3+}, Na^{+}, K^{+}, and Mg^{2+} salts individually. Hydrolysis efficiencies were measured by monitoring soluble COD. It was found that the hydrolysis efficiency was reduced by 50% by the addition of HAs. By the addition of metal Ca^{2+}, Mg^{2+}, and Fe^{3+} along with HAs, the hydrolysis efficiency was reduced only by 6 %, 18%, and 10 % respectively.

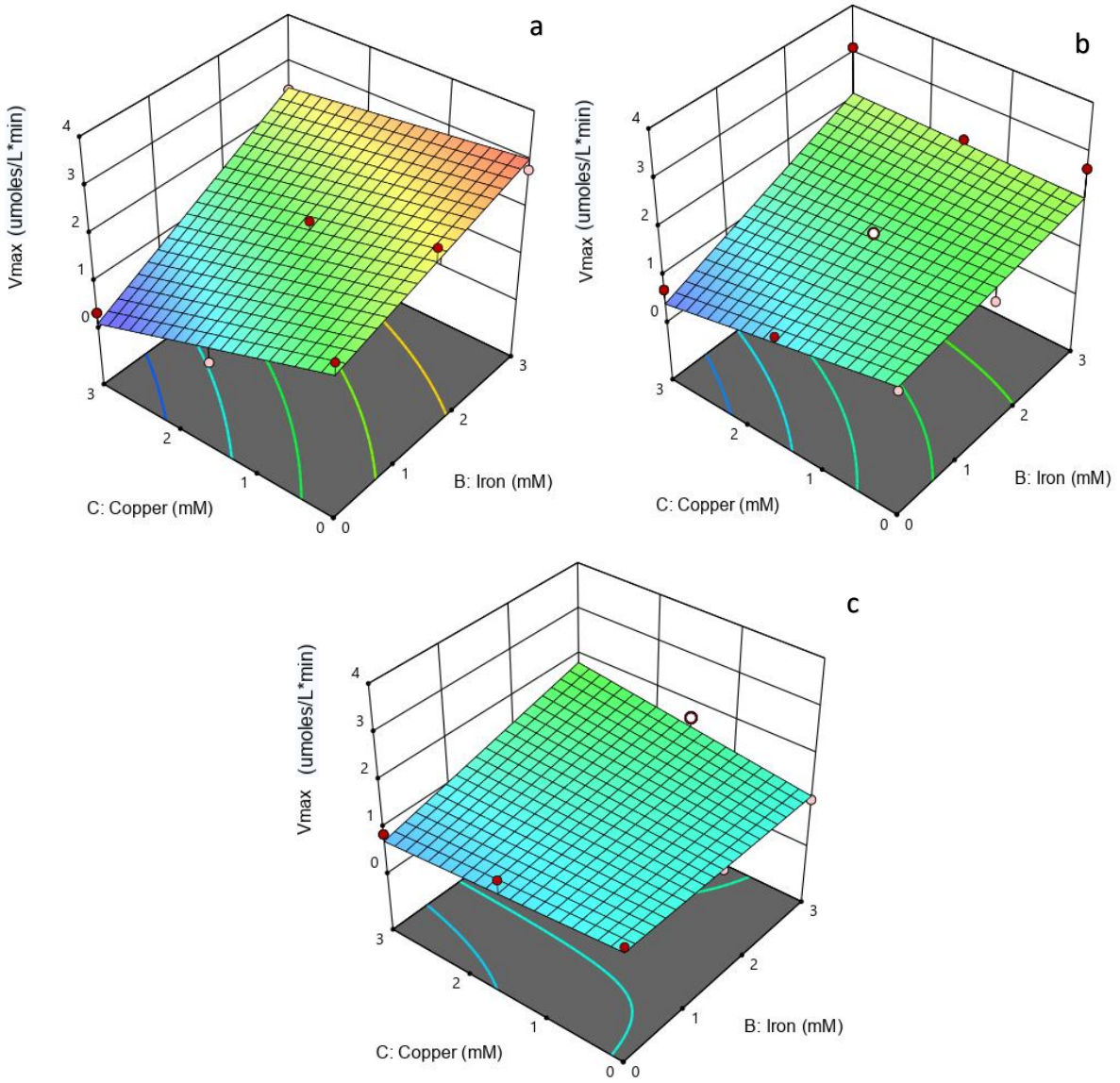

Figure 14: Response surface of Cu^{2+} Vs Fe^{3+} on rate of hydrolysis (V_{max}) at (a) 0 mM melanoidins, (b) 5 mM melanoidins and (c) 10 mM melanoidins

Some of the advantages of surface response methodology are presented in Table 12. The model can be used to study the maximum V_{max} that can be achieved for a given concentration of melanoidins and metals in the system. For example, if a system has 20mM of melanoidins and 2mM of Cu^{2+} and Fe^{2+} than the maximum rate of hydrolysis that could be achieved was 0.718 µmoles/L*min. Further, it can also be used to calculate the optimum dosing of Fe^{3+} or Cu^{2+} (in a provided range) required to achieve the maximum rate of hydrolysis in the given system with a specified concentration of melanoidins. For example, if a system has 20 mM of melanoidins, to achieve a maximum rate of hydrolysis, 4.454 mM Fe^{3+} and 4.874 mM of Cu^{2+} needs to be added to the system. The V_{max} then achieved would be 2.766 µmoles/L*min.

Table 12: Response Surface for Optimal study

Parameter A: Melanoidins (mM)	**Parameter B:** Fe (mM)	**Parameter C:** Copper (mM)	**Response 1:** V_{max} (µmoles/L*min)
20	2	2	**0.718**
20	**4.454**	**4.874**	**2.766**

4.3.2 Proteins Hydrolysis

Hydrolysis of proteins at the maximum concentration of 10mM melanoidins,3mM Fe^{3+}, and Cu^{2+} showed complete inhibition of hydrolysis in the presence of metals (raw results shown in Annexure 4). The protease showed no activity at these concentrations therefore the test was conducted again with concentration diluted 20 times. The maximum concentration of melanoidins tested was 0.5mM while that of metals were 0.15mM.

Similar to hydrolysis of cellulose, the maximum rate of hydrolysis (V_{max}) for the 32 experiments run as per the 3-Level factorial design was calculated and is presented in Table 13. As seen the results indicated that the maximum V_{max} achieved was 0.229 µmoles/L * min with 0.5 mM melanoidins and 0 mM Fe^{3+} and Cu^{2+}, while the minimum V_{max} was 0.041 µmoles/L * min with 0.25mM melanoidins and 0.075 mM Fe^{3+} and Cu^{2+}.

Table 13: Maximum rate of hydrolysis (V_{max}) for the 3-level factorial design

Run	**Parameter A:** Melanoidins (mM)	**Parameter B:** Iron (mM)	**Parameter C:** Copper (mM)	**Response 1:** V_{max} (µmoles/L*min)
1	0.5	0.075	0.075	0.093
2	0.25	0.075	0.075	0.041
3	0.25	0.15	0.075	0.110
4	0	0.15	0.075	0.199
5	0.25	0.075	0.15	0.064
6	0.5	0.075	0.15	0.087
7	0	0	0.15	0.065
8	0.5	0	0.15	0.091
9	0.5	0	0	0.229
10	0	0.15	0	0.137
11	0.25	0.075	0.075	0.080
12	0	0.15	0.15	0.161
13	0.25	0.15	0.15	0.081
14	0.25	0	0.15	0.079
15	0.25	0.075	0	0.177
16	0.25	0	0.075	0.113
17	0.5	0.15	0.075	0.124
18	0	0.075	0	0.168
19	0.5	0	0.075	0.100
20	0.25	0.075	0.075	0.094
21	0	0	0.075	0.101

Run	Parameter A: Melanoidins (mM)	Parameter B: Iron (mM)	Parameter C: Copper (mM)	Response 1: V_{max} (µmoles/L*min)
22	0	0.075	0.075	0.103
23	0.25	0.075	0.075	0.105
24	0.25	0.075	0.075	0.102
25	0	0	0	0.168
26	0.25	0.075	0.075	0.089
27	0.5	0.075	0	0.181
28	0.5	0.15	0.15	0.144
29	0	0.075	0.15	0.061
30	0.5	0.15	0	0.124
31	0.25	0	0	0.184
32	0.25	0.15	0	0.151

Further statistical analysis on V_{max} was using ANOVA and response curves were obtained as explained in section 4.3.1. The quadratic model with an F-value of 10.22 and a p-value of < 0.0001 was chosen. The lack-of-fit test for the selected quadratic model showed non-significance with an F-value of 1.28 and a p-value of 0.4226 implying that the model was a good fit for the experimental V_{max} values.

Table 14 presents the F-value test for each independent variable of the quadratic model (A-Melanoidins, B-Iron, C-copper, A^2, B^2, C^2, AB, AC, and BC) and their significance in terms of the p-value. Variables C, AB, BC, B^2, C^2 are significant model terms with p-values less than 0.05. While the variables B, C, AC, and C^2 are insignificant model terms with very high p-values of 0.93, 0.37, 0.78, and 0.12 respectively. Therefore, the model reduction was done to improve the model, and terms AB and C^2 were eliminated from the model. Terms B and C could not be removed as they are needed to support the hierarchy of the model. This implied that though the concentration of melanoidins and Fe^{3+} were included in the model, it does not have a real impact on the response (V_{max}) individually. Further the R^2 and the adjusted R^2 of the model where 0.75 and 0.68 respectively which illustrated a good correlation between the independent variables and V_{max}.

The regression coefficients of the model terms are also provided in Table 14. The coefficients of the significant terms Cu^{2+}, AB, BC, B^2, C^2 are -0.038, -0.016, 0.027, 0.023 and 0.021. This indicates that Cu^{2+} has a negative impact on V_{max} which might again be due to the inactivation of protease by binding to the active sites. On the other hand, Fe^{3+} individually does not affect the V_{max} but in presence of melanoidins, it reduces the rate of hydrolysis. However, the significance of this occurring is 4.2%.

Table 14: Analysis of Variance for Quadratic model

Source	F-value	p-value		Regression Coefficient
Model	10.22	< 0.0001	Significant	
A-Melanoidin	0.0071	0.9335	Not significant	0.0005
B-Iron	0.8384	0.369	Not significant	0.0056
C-Copper	39.03	< 0.0001		-0.0381
AB	4.59	0.0425		-0.0160
AC	**0.0813**	**0.7789**	**Not significant**	**Eliminated**
BC	12.89	0.0015		0.0268
A^2	**2.69**	**0.1152**	**Not significant**	**Eliminated**
B^2	5.73	0.0248		0.0228
C^2	5.07	0.0338		0.0214
Lack of Fit	1.28	0.4226	Not significant	
R^2	0.7488			
Adjusted R^2	0.6755			
Predicted R^2	0.5142			

Figure 15 shows the Response surface of the combined effect of Cu^{2+}, Fe^{3+}, and melanoidins on the rate of hydrolysis of proteins. It was clear from Figure 15(a) (with 0 mM melanoidins) that the rate of hydrolysis decreases with an increase in Cu^{2+} concentration. The minimum V_{max} for this system is achieved when the concentration of Cu^{2+} is maximum and Fe^{3+} and melanoidins are 0mM. While Figure 15(b) (with 0.5 mM melanoidins) shows the maximum possible V_{max} of the system is achieved with 0mM Cu^{2+} and Fe^{3+} concentration and 0.5 mM melanoidins concentration.

This shows that the protease used in the study is very sensitive to metals and its activity is inhibited in the presence of metals - with a higher impact of Cu^{2+} and lower inhibition by Fe^{3+}. While melanoidins to some extent have a positive impact on the rate of hydrolysis with the regression coefficient of 0.005 but the melanoidins terms in this model are highly non-significant.

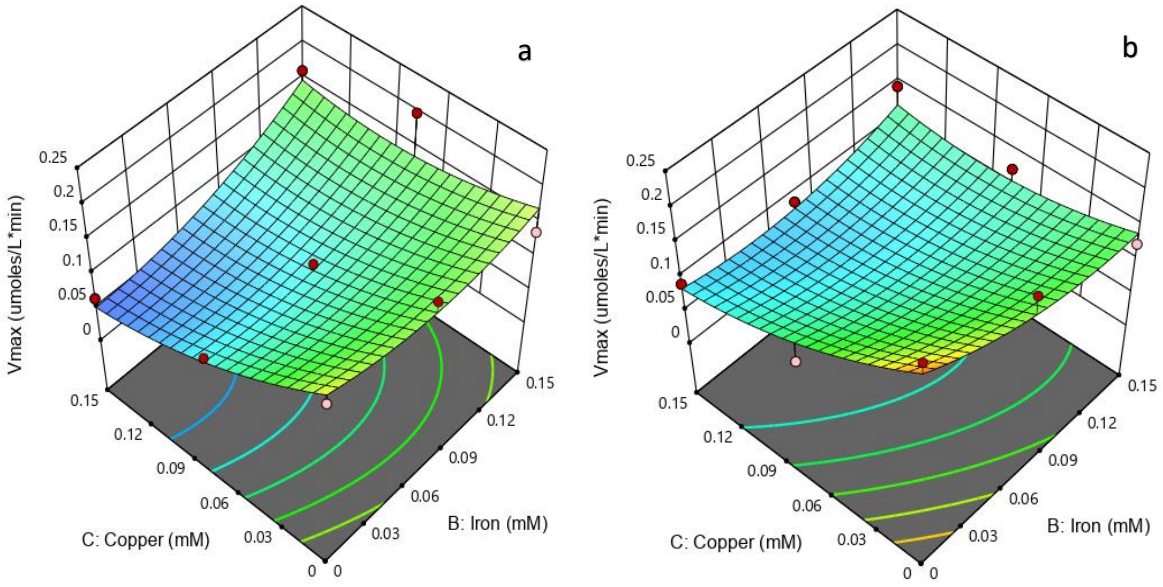

Figure 15: Response surface of Cu^{2+} Vs Fe^{3+} on rate of hydrolysis (V_{max}) at (a) 0 mM melanoidins and (b) 0.5 mM melanoidins

4.4 The mechanism in which Melanoidins interfere in Hydrolysis

4.4.1 Interaction between Enzyme and melanoidins

Ladd & Butler (1970) explained that HAs reversibly bind enzymes by a cation-exchange mechanism causing inhibition of enzymic activity. Similar inhibition by melanoidins on the hydrolysis of cellulose was observed in this study as presented in section 4.3.1. To understand the inhibition mechanism of melanoidins SEC-HPLC chromatograms of melanoidins, cellulase, and a solution of both in the same concentrations as used in the hydrolysis experiments were studied. The chromatograms at 210 nm are presented in Figure 16.

The cellulases contain amino acids and have low aromaticity due to which absorption peaks are observed at 210 nm as in the case of proteins (Her et al., 2008). The ratio UVA_{210}/UVA_{254} of the cellulases was 39.65 at the peak observed at elusion time of 5.6 min. This UVA_{210}/UVA_{254} ratio is comparable to UVA_{210}/UVA_{254} of Bovine Serum Albumin (BSA) protein tested which was 51.70 (chromatograms not shown here). The peak at 8.98 min and 10.70 min are that of acetate buffer which was used as a buffer for experiments of hydrolysis of cellulose. The melanoidins which show absorbance at 210 nm are mostly the proteinaceous melanoidins with the presence of amino groups.

It is observed that the melanoidins are reduced in size in the presence of cellulase. The reduction in the MW is not due to lag in time as the peaks of acetate buffer at 10.70 min coincide in all the chromatograms excluding the possibility of lag in elution. A similar test of melanoidins when conducted with BSA instead of cellulases, no shift in the peaks of the melanoidins was observed. There was no interaction between BSA and melanoidins peaks.

Therefore, it can be concluded that melanoidins are reduced in size in the presence of cellulases due to breakage of the glycosidic bonds which could be incorporated in the melanoidins structure. As per the studies of Cammerer et al. (2002), a significant amount of di- and oligomer carbohydrates were incorporated into the melanoidins skeleton as complete oligomer with intact glycosidic bond, forming side chains at the melanoidin skeleton when the Millard reaction takes place in water-free conditions.

Though this phenomenon decreases when the Millard reaction takes place in aqueous conditions a small quantity of glucose was still released after hydrolysis of these melanoidins (Cammerer et al., 2002). However, no interaction between the cellulase and melanoidins was observed in terms of an increase in MW and the intensity of absorbance.

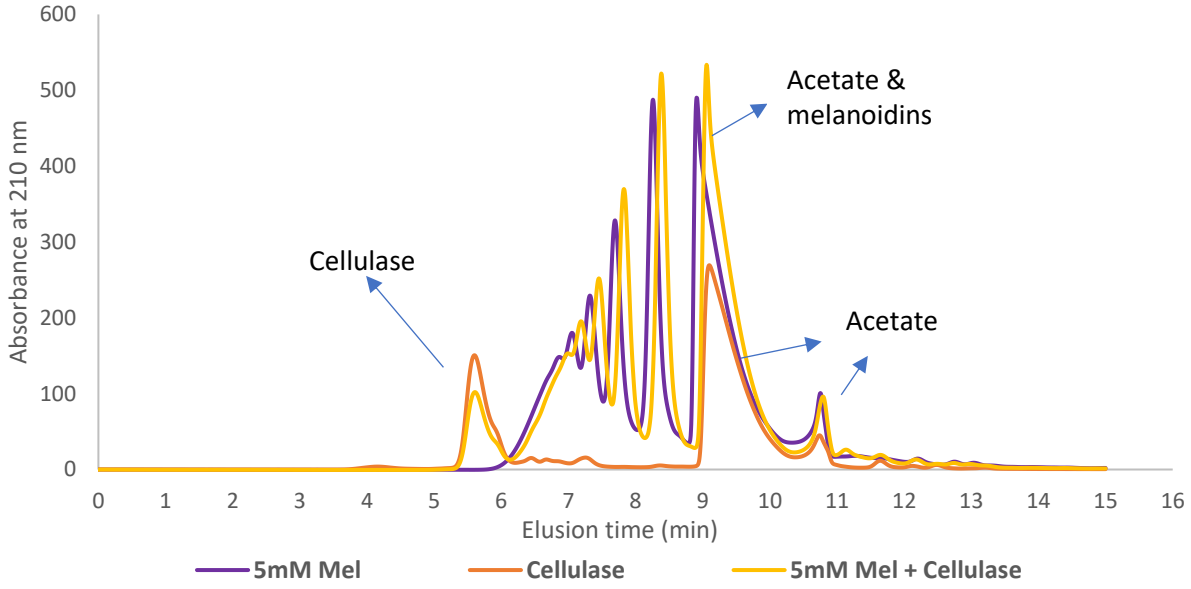

Figure 16: SEC-HPLC chromatograms to evaluate the interaction of melanoidins with Cellulase

4.4.2 Interaction between Enzyme, substrate, and metals

Figure 17 represents the chromatogram of the substrate, cellulase, and a solution of substrate and cellulase with Fe^{3+} and Cu^{2+} in the presence of a stop buffer at 210 nm. The stop buffer used was Tris Buffer at pH 9. The peaks observed at 11.7 min are that of substrate cellobiose used in the study with the MW of 250 Da. The cellulase's peak was observed at 5.6 min while the peak observed at 8.98 min and 10.70 min are that of acetate buffer.

The shift of the substrate peak towards the right in the presence of cellulases was assumed to be due to the hydrolysis of some substrate which leads to a reduction in the size of the substrate. The decrease in the absorbance by cellulase (as shown in the magnified image) could be due to the inactivation of cellulase in the presence of a stop buffer. Lozano et al. (1997) studied the deactivation of enzymes due to temperature and pH which was associated with structural changes of the proteins. With an increase in pH, the denaturation of the enzyme increased, which lead to a decrease in absorbance intensity and change in absorbance wavelength (Lozano et al., 1997).

The absorbance by cellulase in the presence of Fe^{3+} shows a reduction, while there is no absorbance by cellulase in the case of Cu^{2+} as can be seen from the magnified image in Figure 17. This might be due to structural change in the cellulase caused by an increase in pH. The deactivation of the enzyme is more severe with Cu^{2+}, as Cu^{2+} also leads to the inactivation of the enzyme as hypothesised in section 4.3.1 for the hydrolysis of cellulose.

It was also hypothesised that Fe^{3+} improves the rate of hydrolysis by facilitating substrate-enzyme interaction but no such changes in terms of MW are observed in the results presented in Figure 17. The absorbance shown by the substrate is completely separated from that shown by cellulase.

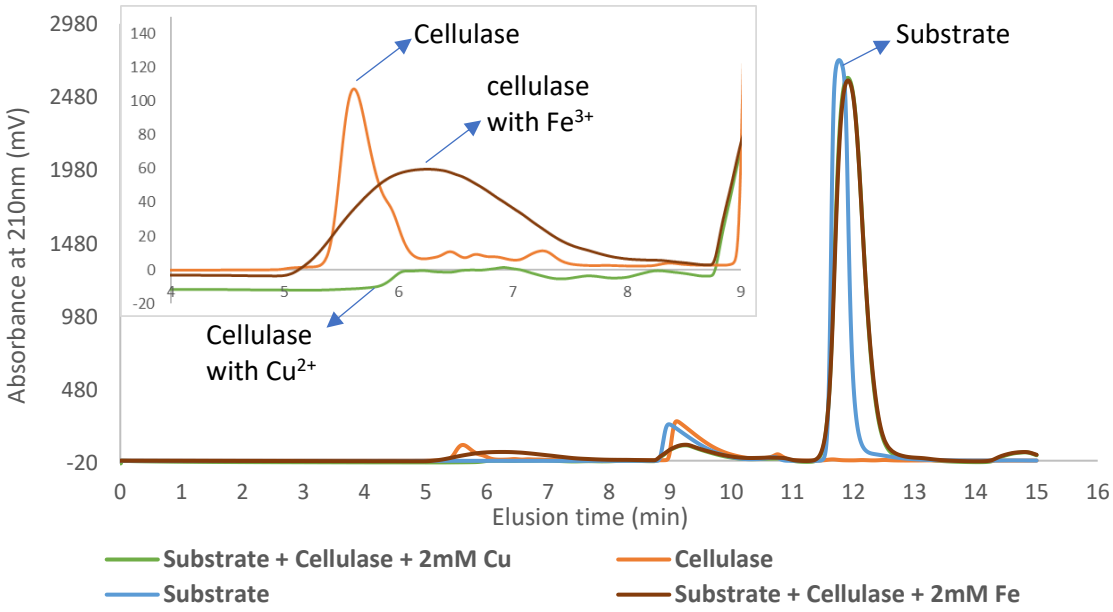

Figure 17: SEC-HPLC chromatograms to evaluate the interaction of substrate and Cellulase in the presence of metals Fe^{3+} and Cu^{2+}

Similarly, the test was then conducted in the presence of melanoidins in the same concentrations as used in the hydrolysis of cellulose. The chromatograms are presented in Figure 18 below. The chromatograms of melanoidins, substrate, and cellulases are provided as a reference to the changes that occur in the solution with melanoidins+ substrate + cellulase + metal (Fe^{3+} or Cu^{2+}) and a stop buffer.

The results showed a shift of the substrate peak towards the right indicating some hydrolysis. However, no such shift was observed in the case of melanoidins indicating that in the presence of substrate the cellulases only hydrolyse the substrate and not melanoidins as seen in Figure 16. The complete disappearance of cellulase peaks (observed in the magnified image) in presence of stop buffer and metals is likely due to the denaturation of enzyme proteins. Also, an increase in the MW of melanoidins is observed in the presence of Fe^{3+} due to melanoidins-Fe^{3+} interaction.

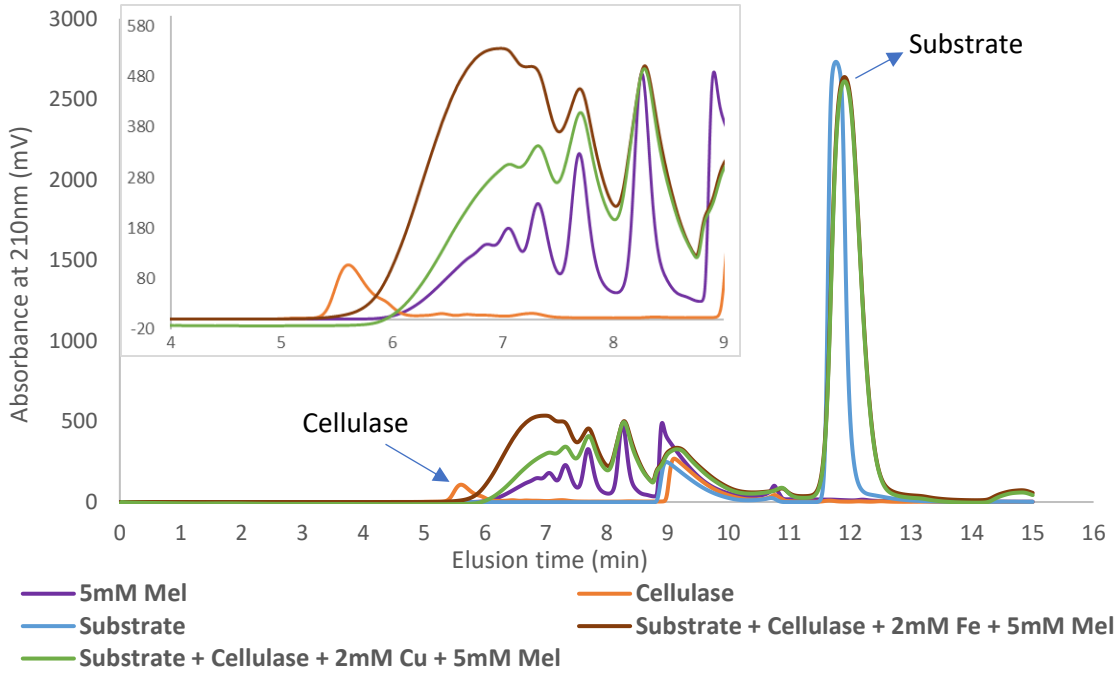

Figure 18: SEC-HPLC chromatograms to evaluate the interaction of substrate, cellulase, and melanoidins in the presence of metals Fe^{3+} and Cu^{2+}

4.5 General Discussion

In this study, it is hypothesised that "melanoidins bind to the active sites of enzymes, inhibiting the hydrolytic activity, melanoidins-metal complexes formation reduces the binding capacity of melanoidins to enzymes and increasing the rate of hydrolysis ".

The results from the first research question clearly indicate that melanoidins form complexes with di-valent metals Ca^{2+}, Mg^{2+}, Cu^{2+} and Fe^{2+}. The results from the second research question show the rate of hydrolysis was decreased in presence of melanoidins, Cu^{2+} had an inhibiting effect on the rate of hydrolysis while Fe^{3+} increased the rate of hydrolysis. Therefore, as per the hypothesis, in presence of melanoidins, the rate of hydrolysis should improve with addition of metals concentration as all the metals tested form complexes with melanoidins.

However, in presence of melanoidins, Ca^{2+} does not show any significant impact on the rate of hydrolysis. As shown in Figure 19, in presence of 3mM Cu^{2+}, the rate of hydrolysis is higher with 10 mM melanoidins rather than 0 mM melanoidins pointing to the fact that melanoidins-Cu^{2+} complexes lead to non-availability of Cu^{2+} for enzyme inhibition thus improving rate of hydrolysis. While, Fe^{3+} shows no increase/decrease in the rate of hydrolysis in presence of 10 mM melanoidins as seen in Figure 19.

Furthermore, in presence of melanoidins, the rate of hydrolysis is maximum with highest concentration (3mM) of Cu^{2+} and Fe^{3+}. It is probably due to utilization of Cu^{2+} and melanoidins binding sites for formation of melanoidins-Cu^{2+} complexes which makes Cu^{2+} unavailable for enzyme inhibition, melanoidins functional groups unavailable for Fe^{3+} complexation and thus more freely available Fe^{3+} ions for enzyme activation.

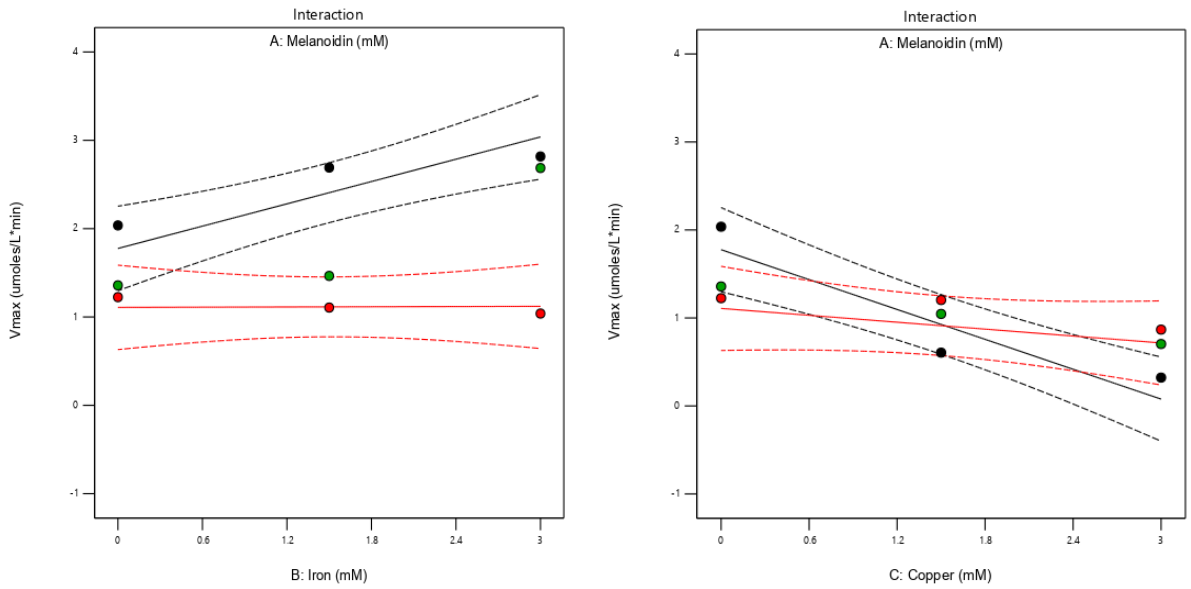

Figure 19: Interaction effect of melanoidins and metals Fe^{3+} and Cu^{2+} on rate of hydrolysis (Black line is 0 mM melanoidins, red line is mM melanoidins)

Further, the results from the third research question showed some breakage of glycosidic bonds present in the melanoidins structure by cellulases but no interaction between melanoidins and enzymes in terms of MW (binding of melanoidins to the active enzyme site) and absorbance at 210 nm was observed.

Therefore, it is hypothesised that the change in rate of hydrolysis in co-presence of melanoidins and metals might not be due to non-availability of melanoidins to bind to the active sites of enzymes, but is predicted to be due to non-availability of metals which are primarily responsible for the inhibition and acceleration of hydrolysis by formation of melanoidins-metals complexes.

5

Recommendations

The study uses various experimental and statistical methods to investigate the effect of melanoidins and metals on hydrolysis. This chapter provides some recommendations to improve the experimental methods used in this study and further research that could provide a better insight into the research.

SEC-HPLC coupled with ICP-MS was used to study the interactions of melanoidins with cations. Loss of metals was observed either due to the sample collection method or due to chloride ions interaction with the column. The elusion profile of melanoidins using UV detection can be compared with those from ICPMS detection of metals in the same chromatographic runs (Wrobel et al., 2003). In this coupled technique, SEC would provide a relatively simple and convenient means for studying apparent MW distribution of melanoidins, while element-specific detection would assure highly selective and specific information for individual elements from one chromatographic run. This could be used to study the extent to which a metal lead to intra-molecular complexation or inter-molecular interaction (aggregation) of melanoidins. It can provide very detailed information on the role of MW of melanoidins on complexation with metals.

In this study, fluorescence was used to evaluate the rate of hydrolysis in the presence of melanoidins and metals. It was clear that the decay of fluorescence over time was linearly dependent on the product concentration. Therefore, to correct for the underestimation of V_{max} calculated from florescence change over time, the K_d (decay coefficient) was evaluated. However, the decay could also be time-dependent or dependent on both product concentration and time simultaneously. The effect of K_d should then be included in the Michaels-Menten model to solve the ODE and achieve the best fit for the experimental data and thus obtain the values of K_s by the non-linear fitting. The MATLAB code written till date to achieve this is provided in Annexure 5, however, a perfect fit for the experimental data is not yet achieved in the study and needs further evaluation.

More metals that are commonly found in WWTP such as Ca^{2+} and Mg^{2+} could also be tested simultaneously using surface response methodology design such as Box and Behnken. Box and Behnken design are more efficient and economical then 3-level factorial designs for many variables. Then, to further optimize the studies again 3-level factorial designs or Central composite design could be used. This could be an optimum way to then evaluate the rate of hydrolysis in any AD system with the model generated.

Further, to understand the impact of melanoidins and metals on AD of WAS, it is important to conduct hydrolysis test on lipids as 10% of the WAS consists of lipids. There is a scope of improvement in the test conducted for hydrolysis of proteins. Enzymes that are not completely inactivated by metals could be used to obtain results in the range of metals used in the study.

The generalisability of findings in the cellulose and protein hydrolysis test is limited, as the test was conducted with one enzyme only. Many studies have reported different effects of the same metal and organic matter on the activity of enzymes secreted by different micro-organisms (Pereira et al., 2012). Therefore, it is important to study the effect of melanoidins and metals on enzymes extracted from

the EPS of the sludge as this would then be a combination of enzymes generated by the hydrolytic, fermentative, and methanogenic bacteria which could be much more robust then commercially available enzymes.

HAs extracted from the THP system could be used further as they could have higher MW and with different characteristics than melanoidins could thus have a different impact on the rate of hydrolysis. To have a better understanding of the mechanism that takes a role in the change of the rate of hydrolysis in the co-presence of melanoidins/HAs, it is very important to characterise the HAs used in terms of aromaticity, amount of carboxyl, hydroxyl and phenolic functional groups. Various methods can be used for this purpose such as ^{13}C NMR spectra, Fourier Transform Infrared Spectroscopy (FTIR) analysis.

Lastly, the research could be done on a pilot scale to find the effect of melanoidins and metals on the bacterial mass. In an AD system, the enzymes are generated by bacteria present in the system and thus it is important to not only find the effect of melanoidins and metals on enzymes but also on the bacteria that secrete the enzymes.

6

Conclusion

AD of WAS is a favoured sludge stabilisation technique due to its low energy footprint. Hydrolysis, the first step of AD is often the rate limiting step of AD and thus pre-treatment such as THP are implemented with AD. The application of THP leads to an increase in recalcitrant compounds such as melanoidins and release of heavy metals incorporated in sludge flocs by degradation of EPS structures with increase in temperature. Therefore, the aim of this study was to understand the effect of melanoidins and metals on hydrolysis step in AD by answering three main research objectives : 1) do melanoidins and cations interact 2) what is the effect of presence of melanoidins and metals on hydrolysis of cellulose and proteins 3) what is the inhibition mechanism of melanoidins in hydrolysis. The conclusions drawn from the study are:

- The complexation of melanoidins with cations follow the trend $Fe^{2+} > Ca^{2+} > Mg^{2+} > Cu^{2+} > K^{+} \geq NH_4^{+}$. The ions with higher charge and ionic radius interacted with melanoidins more effectively. The melanoidins-metal interaction increased with increase in melanoidins concentration most likely due to availability of more phenolic and carboxylic functional groups for binding. The melanoidins-metal interaction decreased with increase in metal concentration due to increase in the ionic strength of the solution and saturation of available binding sites in melanoidins.
- Fe^{3+} had a higher binding capacity which lead to charge neutralisation and thus inter-molecular complexation with increase the MW of melanoidins, while Cu^{2+} and Ca^{2+} lead to intra-molecular complexes due to residual charge on melanoidins with no evident increase in MW.
- When present individually, increased Fe^{3+} concentration increases rate of hydrolysis of cellulose, increased Cu^{2+} concentration decreases rate of hydrolysis and increased melanoidins concentration decreases rate of hydrolysis.
- In presence of melanoidins, rate of hydrolysis was improved at higher concentrations of both metals Cu^{2+} and Fe^{3+}. It was hypothesised that Cu^{2+} inhibits hydrolysis by inactivating cellulases, but in presence of melanoidins it facilitated hydrolysis by forming melanoidins- Cu^{2+} complexes thus negating its toxic effect on cellulases. While, Fe^{3+} improved hydrolysis by facilitating substrate-enzyme interaction but in presence of melanoidins, melanoidins-Fe^{3+} complexation lead to non-availability of Fe^{3+} to facilitate hydrolysis process thus having no major impact on rate of hydrolysis.
- Protein hydrolysis was completely inhibited with 3mM metals concentration. When tested with 0.15mM metals, it was observed that melanoidins and Fe^{3+} had no major impact on the rate of hydrolysis while Cu^{2+} inhibited hydrolysis.
- It was assumed that melanoidins inhibit hydrolysis of cellulose by binding to the active sites of enzymes, however no increase in MW was observed in SEC-HPLC chromatograms and thus no definitive proof of this could be presented.

References

Ahcllar, A., Meriç, G., Akkurt, F., & Olcay, Ş. (2016). Air Oxidation of Ferrous Iron in Water. *Journal of International Environmental Application and Science*, *8*(5), 409–414.

Alpatova, A., Verbych, S., Bryk, M., Nigmatullin, R., & Hilal, N. (2004). Ultrafiltration of water containing natural organic matter: Heavy metal removing in the hybrid complexation-ultrafiltration process. *Separation and Purification Technology*, *40*(2), 155–162. https://doi.org/10.1016/j.seppur.2004.02.003

APHA. (1992). *Standard Methods for the Examination of Water and Wastewater* (18th ed.). American Public Health Association.

Appels, L., Baeyens, J., Degrève, J., & Dewil, R. (2008). Principles and potential of the anaerobic digestion of waste-activated sludge. *Progress in Energy and Combustion Science*, *34*(6), 755–781. https://doi.org/10.1016/j.pecs.2008.06.002

Appels, L., Degrève, J., Van der Bruggen, B., Van Impe, J., & Dewil, R. (2010). Influence of low temperature thermal pre-treatment on sludge solubilisation, heavy metal release and anaerobic digestion. *Bioresource Technology*, *101*(15), 5743–5748. https://doi.org/10.1016/j.biortech.2010.02.068

Asakawa, D., Iimura, Y., Kiyota, T., Yanagi, Y., & Fujitake, N. (2011). Molecular size fractionation of soil humic acids using preparative high performance size-exclusion chromatography. *Journal of Chromatography A*, *1218*(37), 6448–6453. https://doi.org/10.1016/j.chroma.2011.07.030

Azman, S. (2016). *Anaerobic digestion of cellulose and hemicellulose in the presence of humic acids* (Issue January).

Azman, S., Khadem, A. F., Zeeman, G., van Lier, J. B., & Plugge, C. M. (2015). Mitigation of humic acid inhibition in anaerobic digestion of cellulose by addition of various salts. *Bioengineering*, *2*(2), 54–65. https://doi.org/10.3390/bioengineering2020054

Barber, W. P. F. (2016). Thermal hydrolysis for sewage treatment: A critical review. *Water Research*, *104*, 53–71. https://doi.org/10.1016/j.watres.2016.07.069

Batstone, D. J., Keller, J., Newell, R. B., & Newland, M. (2000). Modelling anaerobic degradation of complex wastewater. I: Model development. *Bioresource Technology*, *75*(1), 67–74. https://doi.org/10.1016/S0960-8524(00)00018-3

Blondeau, R. (1989). Biodegradation of Natural and Synthetic Humic Acids by the White Rot Fungus Phanerochaete chrysosporium. *Applied and Environmental Microbiology*, *55*(5), 1282–1285. https://doi.org/10.1128/aem.55.5.1282-1285.1989

Bougrier, C., Delgenès, J. P., & Carrère, H. (2007). Impacts of thermal pre-treatments on the semi-continuous anaerobic digestion of waste activated sludge. *Biochemical Engineering Journal*, *34*(1), 20–27. https://doi.org/10.1016/j.bej.2006.11.013

Bougrier, C., Delgenès, J. P., & Carrère, H. (2008). Effects of thermal treatments on five different waste activated sludge samples solubilisation, physical properties and anaerobic digestion. *Chemical Engineering Journal*, *139*(2), 236–244. https://doi.org/10.1016/j.cej.2007.07.099

Branden, C., & Tooze, J. (1999). The Building Blocks of Proteins. In *Introduction to Protein Structure* (Second, pp. 1–12). Garland Science, Taylor and Francis Group.

Brons, H. J., Field, J. A., Lexmond, W. A. C., & Lettinga, G. (1985). Influence of humic acids on the hydrolysis of potato protein during anaerobic digestion. *Agricultural Wastes*, *13*(2), 105–114. https://doi.org/10.1016/0141-4607(85)90017-4

Butler, J. H. A., & Ladd, J. N. (1971). Importance of the molecular weight of humic and fulvic acids in determining their effects on protease activity. *Soil Biology and Biochemistry*, *3*(3), 249–257. https://doi.org/10.1016/0038-0717(71)90021-6

Cammerer, B., Jalyschko, W., & Kroh, L. W. (2002). Intact Carbohydrate Structures as Part of the Melanoidin Skeleton. *Agriculture and Food Chemistry*, *50*, 2083–2087.

Cheng, W. P. (2002). Comparison of hydrolysis/coagulation behavior of polymeric and monomeric iron coagulants in humic acid solution. *Chemosphere*, *47*(9), 963–969.

https://doi.org/10.1016/S0045-6535(02)00052-8

Christl, I., & Kretzschmar, R. (2001). Relating ion binding by fulvic and humic acids to chemical composition and molecular size. 1. Proton binding. *Environmental Science and Technology*, *35*(12), 2505–2511. https://doi.org/10.1021/es0002518

Climent, M., Ferrer, I., Baeza, M. del M., Artola, A., Vázquez, F., & Font, X. (2007). Effects of thermal and mechanical pretreatments of secondary sludge on biogas production under thermophilic conditions. *Chemical Engineering Journal*, *133*(1–3), 335–342. https://doi.org/10.1016/j.cej.2007.02.020

de Oliveira, F. C., Coimbra, J. S. dos R., de Oliveira, E. B., Zuñiga, A. D. G., & Rojas, E. E. G. (2016). Food Protein-polysaccharide Conjugates Obtained via the Maillard Reaction: A Review. *Critical Reviews in Food Science and Nutrition*, *56*(7), 1108–1125. https://doi.org/10.1080/10408398.2012.755669

Dewil, R., Baeyens, J., & Appels, L. (2007). Enhancing the use of waste activated sludge as bio-fuel through selectively reducing its heavy metal content. *Journal of Hazardous Materials*, *144*(3), 703–707. https://doi.org/10.1016/j.jhazmat.2007.01.100

Dwyer, J., Starrenburg, D., Tait, S., Barr, K., Batstone, D. J., & Lant, P. (2008). Decreasing activated sludge thermal hydrolysis temperature reduces product colour, without decreasing degradability. *Water Research*, *42*(18), 4699–4709. https://doi.org/10.1016/j.watres.2008.08.019

Eastman, J. A., & Ferguson, J. F. (1981). Solubilization organic phase of of carbon anaerobic particulate during the digestion acid. *Journal (Water Pollution Control Federation)*, *53*(3), 352–366.

EEA. (2018). *Environmental indicator report 2018 - Waste generation*.

Fernandes, T. V. (2010). *Hydrolysis inhibition of complex biowaste*. 176.

Fernandes, T. V., van Lier, J. B., & Zeeman, G. (2015). Humic Acid-Like and Fulvic Acid-Like Inhibition on the Hydrolysis of Cellulose and Tributyrin. *Bioenergy Research*, *8*(2), 821–831. https://doi.org/10.1007/s12155-014-9564-z

Fischer, E. (1894). Einfluss der Configuration auf die Wirkung der Enzyme. *Ber. Dtsch. Chem. Ges.*, *27*, 2985–2993.

Gallert, C., & Winter, J. (2008). Bacterial Metabolism in Wastewater Treatment Systems. In *Biotechnology: Second, Completely Revised Edition* (Vols. 11–12). https://doi.org/10.1002/9783527620999.ch2l

Gerardi, M. H. (2003). *The Microbiology of Anaerobic Digesters*. John Wiley & Sons, Inc.

Godbey, W. T. (2014). Chapter 2 - Proteins. In *An Introduction to Biotechnology* (pp. 9–33). Elsevier Ltd. https://doi.org/10.1016/B978-1-907568-28-2.00002-2

Goel, R., Mino, T., Satoh, H., & Matsuo, T. (1998a). COMPARISON OF HYDROLYTIC ENZYME SYSTEMS IN PURE CULTURE AND ACTIVATED SLUDGE UNDER DIFFERENT ELECTRON ACCEPTOR CONDITIONS. *Water Science and Technology*, *37*(4–5), 335–343. https://doi.org/10.1016/S0273-1223(98)00126-7

Goel, R., Mino, T., Satoh, H., & Matsuo, T. (1998b). Enzyme activities under anaerobic and aerobic conditions in activated sludge sequencing batch reactor. *Water Research*, *32*(7), 2081–2088. https://doi.org/10.1016/S0043-1354(97)00425-9

Gomyo, T., & Horikoshi, M. (1976). On the interaction of melanoidin with metallic ions. *Agricultural and Biological Chemistry*, *40*(1), 33–40. https://doi.org/10.1080/00021369.1976.10862003

Gonzalez, A., Hendriks, A. T. W. M., van Lier, J. B., & de Kreuk, M. (2018). Pre-treatments to enhance the biodegradability of waste activated sludge: Elucidating the rate limiting step. *Biotechnology Advances*, *36*(5), 1434–1469. https://doi.org/10.1016/j.biotechadv.2018.06.001

Gujer, W., & Zehnder, A. J. B. (1983). Conversion processes in anaerobic digestion. *Water Science and Technology*, *15*(8–9), 127–167. https://doi.org/10.2166/wst.1983.0164

Hankins, N. P., Lu, N., & Hilal, N. (2006). Enhanced removal of heavy metal ions bound to humic acid by polyelectrolyte flocculation. *Separation and Purification Technology*, *51*(1), 48–56. https://doi.org/10.1016/j.seppur.2005.12.022

Haug, R. T., Stuckey, D. C., Gossett, J. M., & McCarty, P. L. (1978). Effect of Thermal Pretreatment on Digestibility and Dewaterability of Organic Sludges. *Journal (Water Pollution Control Federation)*, *50*(1), 73–85. http://www.jstor.org/stable/25039508

Her, N., Amy, G., Sohn, J., & Gunten, U. (2008). UV absorbance ratio index with size exclusion chromatography (URI-SEC) as an NOM property indicator. *Journal of Water Supply: Research and Technology - AQUA*, *57*(1), 35–44. https://doi.org/10.2166/aqua.2008.029

Hills, D. J., & Nakano, K. (1984). Effects of particle size on anaerobic digestion of tomato solid wastes. *Agricultural Wastes*, *10*(4), 285–295. https://doi.org/10.1016/0141-4607(84)90004-0

Hobson, P. N. (1987). A model of some aspects of microbial degradation of particulate substrates. *Journal of Fermentation Technology*, *65*(4), 431–439. https://doi.org/10.1016/0385-6380(87)90140-3

Hu, Z. H., Yu, H. Q., & Zhu, R. F. (2005). Influence of particle size and pH on anaerobic degradation of cellulose by ruminal microbes. *International Biodeterioration and Biodegradation*, *55*(3), 233–238. https://doi.org/10.1016/j.ibiod.2005.02.002

Hurst, P. L., Sullivan, P. A., & Shepherd, M. G. (1977). Chemical modification of a cellulase from Aspergillus niger. *Biochemical Journal*, *167*(3), 549–556. https://doi.org/10.1042/bj1670549

Ikram-ul-Haq Mukhtar, H. Ali, Z. R. (2004). Protease biosynthesis by mutant strain of Penicillium griseoroseum and cheese formation. *Pakistan J. Biol. Sci.*, *7*(9), 1473–1476.

Jahnel, J. B., & Frimmel, F. H. (1994). Comparison of the enzyme inhibition effect of different humic substances in aqueous solutions. *Chemical Engineering and Processing*, *33*(5), 325–330. https://doi.org/10.1016/0255-2701(94)02003-5

Jain, S., Lala, A. K., Bhatia, S. K., & Kudchadker, A. P. (1992). Modelling of hydrolysis controlled anaerobic digestion. *Journal of Chemical Technology & Biotechnology*, *53*(4), 337–344. https://doi.org/10.1002/jctb.280530404

Jonke, A., & Michal, G. (2007). Enzymes in Industry: Production and Applications. In W. Aehel (Ed.), *Enzymes in Industry: Production and Applications* (Third, pp. 13-33Jonke, A., Michal, G. (2007). Enzymes in In). WILEY-VCH Verlag GmbH & Co. KGaA.

Junias, A.-G., DUMOULIN, D., Superville, P.-J., Ouddane, B., Heijman, B., Rietveld, L., & CRIQUET, J. (2018). Elimination of natural organic matter and its complexes formed with metallic trace elements in drinking water supply chains. *Journées Information Eaux, APTEN*. https://hal.archives-ouvertes.fr/hal-01919283

Kepp, U., Machenbach, I., Weisz, N., & Solheim, O. E. (2000). Enhanced stabilisation of sewage sludge through thermal hydrolysis - Three years of experience with full scale plant. *Water Science and Technology*, *42*(9), 89–96. https://doi.org/10.2166/wst.2000.0178

Kim, H. J., Baek, K., Kim, B. K., & Yang, J. W. (2005). Humic substance-enhanced ultrafiltration for removal of cobalt. *Journal of Hazardous Materials*, *122*(1–2), 31–36. https://doi.org/10.1016/j.jhazmat.2005.03.043

Koshland, D. E. (1958). Application of a Theory of Enzyme Specificity to Protein Synthesis. *Proceedings of the National Academy of Sciences*, *44*(2), 98–104. https://doi.org/10.1073/pnas.44.2.98

Kuglarz, M., Karakashev, D., & Angelidaki, I. (2013). Microwave and thermal pretreatment as methods for increasing the biogas potential of secondary sludge from municipal wastewater treatment plants. *Bioresource Technology*, *134*, 290–297. https://doi.org/10.1016/j.biortech.2013.02.001

Ladd, J. N., & Butler, J. H. A. (1970). The effect of inorganic cations on the inhibition and stimulation of protease activity by soil humic acids. *Soil Biology and Biochemistry*, *2*(1), 33–40. https://doi.org/10.1016/0038-0717(70)90023-4

Laurent, J., Casellas, M., & Dagot, C. (2009). Heavy metals uptake by sonicated activated sludge: Relation with floc surface properties. *Journal of Hazardous Materials*, *162*(2–3), 652–660. https://doi.org/10.1016/j.jhazmat.2008.05.066

Li, C., & Fang, H. H. P. (2007). Inhibition of heavy metals on fermentative hydrogen production by granular sludge. *Chemosphere*, *67*(4), 668–673. https://doi.org/10.1016/j.chemosphere.2006.11.005

Li, Y. Y., & Noike, T. (2015). Upgrading of anaerobic digestion of waste activated sludge by temperature-phased process with recycle. *Energy*, *87*(34), 381–389. https://doi.org/10.1016/j.energy.2015.04.110

Liu, X., Wang, W., Gao, X., Zhou, Y., & Shen, R. (2012). Effect of thermal pretreatment on the physical and chemical properties of municipal biomass waste. *Waste Management*, *32*(2), 249–255. https://doi.org/10.1016/j.wasman.2011.09.027

Lozano, P., De Diego, T., & Iborra, J. L. (1997). Dynamic structure/function relationships in the α-chymotrypsin deactivation process by heat and pH. *European Journal of Biochemistry*, *248*(1), 80–85. https://doi.org/10.1111/j.1432-1033.1997.00080.x

Martins, S. I. F. S., Jongen, W. M. F., & Boekel, M. A. J. S. Van. (2000). A review of Maillard reaction in food and implications to kinetic modelling Sara. *Trends in Food Science & Technology*, *11*(9–10), 364–373. https://doi.org/10.1515/9783110973976.218

Metcalf, & Eddy. (2014). *Wastewater Engineering Treatment & Resource Recovery* (Fifth). McGraw-Hill Education.

Migo, V. P., Matsumura, M., Del Rosario, E. J., & Kataoka, H. (1993). The effect of pH and calcium ions on the destabilization of melanoidin. *Journal of Fermentation and Bioengineering*, *76*(1), 29–32. https://doi.org/10.1016/0922-338X(93)90048-D

Mojsov, K. D. (2016). Aspergillus Enzymes for Food Industries. In *New and Future Developments in Microbial Biotechnology and Bioengineering: Aspergillus System Properties and Applications*. Elsevier B.V. https://doi.org/10.1016/B978-0-444-63505-1.00033-6

Neyens, E., & Baeyens, J. (2003). A review of thermal sludge pre-treatment processes to improve dewaterability. *Journal of Hazardous Materials*, *98*(1–3), 51–67. https://doi.org/10.1016/S0304-3894(02)00320-5

OKADA, G. (1975). Enzymatic Studies on a Cellulase System of Trichoderma viride: II. Purification and Properties of Two Cellulases1. *The Journal of Biochemistry*, *77*(1), 33–42. https://doi.org/10.1093/oxfordjournals.jbchem.a130717

Pavlostathis, S. G., & Gossett, J. M. (1986). A kinetic model for anaerobic digestion of biological sludge. *Biotechnology and Bioengineering*, *28*(10), 1519–1530. https://doi.org/10.1002/bit.260281010

Pavlostathis, S. G., & Gossett, J. M. (1988). PRELIMINARY CONVERSION MECHANISMS IN ANAEROBIC DIGESTION OF BIOLOGICAL SLUDGES. *Journal of Environmental Engineer*, *114*(3), 575–592.

Pelley, J. W. (2007). *3 - Protein Structure and Function* (J. W. B. T.-E. I. B. Pelley (ed.); pp. 19–28). Mosby. https://doi.org/https://doi.org/10.1016/B978-0-323-03410-4.50009-2

Pereira, J. de C., Ellen Cristine Giese, Moretti, M. M. de S., Gomes, A. C. dos S., Perrone, O. M., Boscolo, M., Silva, R. da, Gomes, E., & Martins, D. A. B. (2012). Effect of Metal Ions, Chemical Agents and Organic Effect of Metal Ions, Chemical Agents and Organic Compounds on Lignocellulolytic Enzymes Activities. *Intech*, *i*(tourism), 13. https://doi.org/10.1016/j.colsurfa.2011.12.014

Pilli, S., Yan, S., Tyagi, R. D., & Surampalli, R. Y. (2015). Thermal pretreatment of sewage sludge to enhance anaerobic digestion: A review. *Critical Reviews in Environmental Science and Technology*, *45*(6), 669–702. https://doi.org/10.1080/10643389.2013.876527

Pino, M. S., Rodríguez-Jasso, R. M., Michelin, M., Flores-Gallegos, A. C., Morales-Rodriguez, R., Teixeira, J. A., & Ruiz, H. A. (2018). Bioreactor design for enzymatic hydrolysis of biomass under the biorefinery concept. *Chemical Engineering Journal*, *347*(March), 119–136. https://doi.org/10.1016/j.cej.2018.04.057

Ruffino, B., Campo, G., Cerutti, A., Zanetti, M., Lorenzi, E., Scibilia, G., & Genon, G. (2016). Preliminary Technical and Economic Analysis of Alkali and Low Temperature Thermo-alkali Pretreatments for the Anaerobic Digestion of Waste Activated Sludge. *Waste and Biomass Valorization*, *7*(4), 667–675. https://doi.org/10.1007/s12649-016-9537-x

Sanders, W. (2001). *Anaerobic hydrolysis digestion of complex substrates*.

Slater, J. C. (1965). Symmetry and Energy Bands in Crystals. In *Quantum Theory of Molecules and Solids.* (Vol. 2). McGraw-Hil.

StatEase. (2020). *StatEase - Design Expert v11*. StatEase.

https://www.statease.com/docs/v11/contents/analysis/fit-summary/

Stevenson, F. J. (1994). *Humus Chemistry: Genesis, Composition, Reactions*. John Wiley & Sons, Inc.

Stuckey, D. C., & McCarty, P. L. (1984). The effect of thermal pretreatment on the anaerobic biodegradability and toxicity of waste activated sludge. *Water Research*, *18*(11), 1343–1353. https://doi.org/10.1016/0043-1354(84)90002-2

Traversi, D., Romanazzi, V., Degan, R., Lorenzi, E., Carraro, E., & Gilli, G. (2015). Microbial-chemical indicator for anaerobic digester performance assessment in full-scale wastewater treatment plants for biogas production. *Bioresource Technology*, *186*, 179–191. https://doi.org/10.1016/j.biortech.2015.03.042

Valo, A., Carrère, H., & Delgenès, J. P. (2004). Thermal, chemical and thermo-chemical pre-treatment of waste activated sludge for anaerobic digestion. *Journal of Chemical Technology and Biotechnology*, *79*(11), 1197–1203. https://doi.org/10.1002/jctb.1106

van Lier, J. B., Mahmound, N., & Zeeman, G. (2008). Anaerobic Wastewater Treatment. In *Biological Wastewatr Treatment:Principles Modelling and Design* (pp. 401–442). IWA Publishing.

Vavilin, V. A., Fernandez, B., Palatsi, J., & Flotats, X. (2008). Hydrolysis kinetics in anaerobic degradation of particulate organic material: An overview. *Waste Management*, *28*(6), 939–951. https://doi.org/10.1016/j.wasman.2007.03.028

Vavilin, V. A., Rytov, S. V., & Lokshina, L. Y. (1996). A description of hydrolysis kinetics in anaerobic degradation of particulate organic matter. *Bioresource Technology*, *56*(2–3), 229–237. https://doi.org/10.1016/0960-8524(96)00034-X

Veeken, A., & Hamelers, B. (1999). Effect of temperature on hydrolysis rates of selected biowaste components. *Bioresource Technology*, *69*(3), 249–254. https://doi.org/10.1016/S0960-8524(98)00188-6

von Wandruszka, R. (2000). Humic acids: Their detergent qualities and potential uses in pollution remediation. *Geochemical Transactions*, *1*(April), 10–15. https://doi.org/10.1039/b001869o

Weemaes, M. P. J., & Verstraete, W. H. (1998). Evaluation of current wet sludge disintegration techniques. *Journal of Chemical Technology and Biotechnology*, *73*(2), 83–92. https://doi.org/10.1002/(SICI)1097-4660(1998100)73:2<83::AID-JCTB932>3.0.CO;2-2

Westerholm, M., & Schnürer, A. (2016). Microbial Responses to Different Operating Practices for Biogas Production Systems. In *Intech* (pp. 1–37). https://doi.org/http://dx.doi.org/10.5772/57353

Whiteley, C. G., & Lee, D. J. (2006). Enzyme technology and biological remediation. *Enzyme and Microbial Technology*, *38*(3–4), 291–316. https://doi.org/10.1016/j.enzmictec.2005.10.010

Wilson, C. A., & Novak, J. T. (2009). Hydrolysis of macromolecular components of primary and secondary wastewater sludge by thermal hydrolytic pretreatment. *Water Research*, *43*(18), 4489–4498. https://doi.org/10.1016/j.watres.2009.07.022

Wrobel, K., Sadi, B. B. M., Wrobel, K., Castillo, J. R., & Caruso, J. A. (2003). Effect of metal ions on the molecular weight distribution of humic substances derived from municipal compost: Ultrafiltration and size exclusion chromatography with spectrophotometric and inductively coupled plasma-MS detection. *Analytical Chemistry*, *75*(4), 761–767. https://doi.org/10.1021/ac0261193

Xue, Y., Liu, H., Chen, S., Dichtl, N., Dai, X., & Li, N. (2015). Effects of thermal hydrolysis on organic matter solubilization and anaerobic digestion of high solid sludge. *Chemical Engineering Journal*, *264*, 174–180. https://doi.org/10.1016/j.cej.2014.11.005

Yates, L. M., & Von Wandruszka, R. (1999). Decontamination of polluted water by treatment with a crude humic acid blend. *Environmental Science and Technology*, *33*(12), 2076–2080. https://doi.org/10.1021/es980408k

Zahmatkesh, M., Spanjers, H., & van Lier, J. B. (2017). Fungal treatment of humic-rich industrial wastewater: application of white rot fungi in remediation of food-processing wastewater. *Environmental Technology (United Kingdom)*, *38*(21), 2752–2762. https://doi.org/10.1080/09593330.2016.1276969

Zeeman, G., Sanders, W. T. M., Wang, K. Y., & Lettinga, G. (1997). Anaerobic treatment of complex wastewater and waste activated sludge — Application of an upflow anaerobic solid removal (UASR) reactor for the removal and pre-hydrolysis of suspended COD. *Water Science and Technology*, *35*(10), 121–128. https://doi.org/10.1016/S0273-1223(97)00210-2

Zhang, B., Zhang, L.-L., Zhang, S.-C., Shi, H.-Z., & Cai, W.-M. (2005). The Influence of pH on Hydrolysis and Acidogenesis of Kitchen Wastes in Two-phase Anaerobic Digestion. *Environmental Technology*, *26*(3), 329–340. https://doi.org/10.1080/09593332608618563

Zhang, S., Guo, H., Du, L., Liang, J., Lu, X., Li, N., & Zhang, K. (2015). Influence of NaOH and thermal pretreatment on dewatered activated sludge solubilisation and subsequent anaerobic digestion: Focused on high-solid state. *Bioresource Technology*, *185*, 171–177. https://doi.org/10.1016/j.biortech.2015.02.050

Annexure 1 (MATLAB Code)

```
% Extracting Raw data
kinetics_filename='Kinetics.xlsx';
blank_filename='Blank.xlsx';
Ref_filename='Reference Std.xlsx';
rawkinetics=readtable(kinetics_filename,'ReadRowNames',true);
rawblank=readtable(blank_filename,'ReadRowNames',true);
rawRef=readtable(Ref_filename,'ReadRowNames',true);
time = str2double(table2array(rawkinetics(30:75,2)));
wells = table2array(rawkinetics(29,4:35));
rfu = str2double(table2array(rawkinetics(30:75,4:35)));
blankT = transpose(table2array(rawblank(29:36,2:5)));
blank = transpose(blankT(:));
Ref1T = transpose(table2array(rawRef(28:35,2:5)));
Ref1 = transpose(Ref1T(:));
Ref2T = transpose(table2array(rawRef(28:35,6:9)));
Ref2 = transpose(Ref2T(:));
Ref3T = transpose(table2array(rawRef(28:35,10:13)));
Ref3 = transpose(Ref3T(:));

% Figure 1: Raw data (RFU Vs Time)
figure (1)
ax=tiledlayout(4,8);
title(ax,'Raw Data - RFU Vs Time')
for i=1:32
nexttile
plot(time, rfu(:,i),'-r')
ylim([0,90000]);
xlim([0,50]);
title(wells(i))
end

% Calibration curve
stdconc = [0.025,0.0125,0.0025];
Ref = zeros(3,32);
for i=1:3
    for j=1:32
        Ref(1,j) = Ref1(1,j) - blank(1,j);
        Ref(2,j) = Ref2(1,j) - blank(1,j);
        Ref(3,j) = Ref3(1,j) - blank(1,j);
    end
end
calidata = zeros(32,2);
fdata = zeros(32,3);
RSdata = zeros (32,1);
for j=1:32
    [cali,S] = polyfit(stdconc,[Ref(1,j),Ref(2,j),Ref(3,j)],1);
    f = polyval(cali,stdconc);
    RS = 1 - (S.normr/norm([Ref(1,j),Ref(2,j),Ref(3,j)] -
mean([Ref(1,j),Ref(2,j),Ref(3,j)])))^2;
    calidata(j,1)=cali(1,1);
    calidata(j,2)=cali(1,2);
    fdata(j,1)=f(1,1);
    fdata(j,2)=f(1,2);
    fdata(j,3)=f(1,3);
    RSdata(j,1)= RS;
end

% Figure 2: Calibration curve (RFU Vs Std Conc)
```

```
figure (2)
ax=tiledlayout(4,8);
title(ax,'Calibration curve - RFU Vs Std Conc')
for i=1:32
    nexttile
    plot(stdconc,[Ref(1,i),Ref(2,i),Ref(3,i)],'o')
    hold on
    plot(stdconc,[fdata(i,1),fdata(i,2),fdata(i,3)],'-')
    ylim([0,85000]);
%     xlabel( 'Concentration', 'Interpreter', 'none' );
%     ylabel( 'RFU', 'Interpreter', 'none' );
    title(wells(i))
end

%Calculating Substrate and Product conc
[a, b]=size(rfu);
Pconc = zeros(a,b);
Sconc = zeros(a,b);
for i=1:b
    for j=1:a
        Pconc(j,i) = ((rfu(j,i) - blank(1,i))-calidata(i,2))/calidata(i,1);
    end
end

%Calculating Rate of hydrolysis
dPdtdata = zeros(a-2,b);
d2Pdtdata = zeros(a-2,b);
for i=1:b
     for j=2:a-1
         dPdt = polyfit([time(j-1) time(j) time(j+1)],[Pconc(j-1,i)
Pconc(j,i) Pconc(j+1,i)],1 );
         dPdtdata(j-1,i) = dPdt(1,1);
         d2Pdt = (Pconc(j+1,i)-2*Pconc(j,i)+Pconc(j-1,i))/((time(j+1)-
time(j))^2);
         d2Pdtdata(j-1,i) = d2Pdt(1,1);
    end
end

% Decrease of florescence with time (kd)
mindPdtdata = zeros(b,2);
mind2Pdtdata = zeros(b,2);
for i=1:b
        [l,m] = min(dPdtdata(:,i));
        mindPdtdata(i,1)= l;
        mindPdtdata(i,2)= m;
        [n,o]= min(d2Pdtdata(m:end,i));
        mind2Pdtdata(i,1)= n;
        mind2Pdtdata(i,2)= o;
end
n_P = zeros(a-2,b);
n_time=zeros(a-2,b);
n_dPdt=zeros(a-2,b);
for i = 1:b
    for j=1:a-2
         if j < mindPdtdata(i,2)
             n_dPdt(j,i)= 0;
             n_P(j,i)= 0;
             n_time(j,i) = 0;
         else
             n_dPdt(j,i) = dPdtdata(j,i);
```

```
            n_P(j,i)= Pconc(j,i);
            n_time(j,i) = time(j,1);
        end
    end
end
kddata = zeros(b,2);
RS2data = zeros (b,1);
for i=1:b
    for j=1:a-2
        if j == mindPdtdata(i,2)
            [kda,S] = polyfit(n_P(j+3:44,i),n_dPdt(j+3:44,i),1);
            RS2 = 1 - (S.normr/norm(n_dPdt(j+1:44,i) -
mean(n_dPdt(j+1:44,i))))^2;
            kddata(i,1)=kda(1,1);
            kddata(i,2)=kda(1,2);
            RS2data(i,1)= RS2;
        end
    end
end

% Figure 3: dPdt Vs P (P Vs time)
figure (3)
ax=tiledlayout(4,8);
title(ax,'Kd Data - dPdt Vs P')
for i=1:32
    for j=1:a-2
        if j == mindPdtdata(i,2)
        nexttile
        plot(n_dPdt(j+3:44,i), n_P(j+3:44,i),'-o')
        end
    end
end

% Calculating Vmax with Kd
for i = 1:b
    [d,f] = max(dPdtdata(:,i));
    Vidata (i,1) = d;
    Vidata(i,2) = f;
    Vm = Vidata(i,1) - (kddata(i,1)* Pconc(f,i));
    Vmax (i,1) = Vm;
end

% Figure 4:(P & S Vs time)
figure (4)
ax=tiledlayout(4,8);
title(ax,'P Conc Vs time')
for i=1:32
    nexttile
    plot(time, Pconc(:,i),'-r')
    ylim([0,0.03]);
    xlim([0,50]);
    title(wells(i))
end
```

Annexure 2 (Preliminary test results with metals Ca^{2+}, Fe^{3+} and Cu^{2+})

Table 15 below presents the V_{max} calculated for the enzymatic hydrolysis test conducted with melanoidins and metals Ca^{2+}, Fe^{3+} and Cu^{2+}. Thorough this test it was clear that Calcium did not have any major impact on the rate of hydrolysis.

Table 15: Maximum rate of hydrolysis (V_{max}) for Michaelis-Menten kinetic model for the 3-level factorial design

Run	**Parameter A:** Melanoidins (mM)	**Parameter B:** Calcium (mM)	**Parameter C:** Iron (mM)	**Parameter D:** Copper (mM)	**Response 1:** V_{max} (µmoles/L*min)
1	0	0	3	1.5	0.0491
2	5	1.5	1.5	1.5	0.0324
3	5	3	1.5	1.5	0.0272
4	5	0	3	0	0.0000
5	0	0	3	0	0.0736
6	5	1.5	0	3	0.0216
7	5	0	1.5	3	0.0215
8	10	1.5	1.5	0	0.0259
9	5	1.5	1.5	1.5	0.0173
10	5	0	3	1.5	0.0170
11	10	3	0	1.5	0.0216
12	10	0	1.5	1.5	0.0188
13	10	3	3	3	0.0261
14	10	0	0	0	0.0256
15	10	3	3	0	0.0187
16	5	0	3	3	0.0198
17	5	1.5	3	3	0.0183
18	5	0	1.5	0	0.0356
19	0	3	1.5	0	0.0535
20	5	1.5	0	0	0.0324
21	10	1.5	0	3	0.0515
22	0	1.5	0	1.5	0.0190
23	5	1.5	1.5	1.5	0.0221
24	0	3	1.5	1.5	0.0316
25	0	0	0	1.5	0.0200
26	10	0	1.5	0	0.0457
27	0	3	3	0	0.0759
28	10	3	0	3	0.0188
29	5	1.5	1.5	1.5	0.0186
30	0	1.5	3	0	0.0890
31	5	0	0	3	0.0201
32	0	1.5	0	0	0.0602
33	10	1.5	3	3	0.0186
34	5	3	3	3	0.0038

35	0	0	0	3	0.0119
36	5	0	1.5	1.5	0.0199
37	5	1.5	3	1.5	0.0305
38	10	1.5	3	1.5	0.0236
39	5	3	3	1.5	0.0202
40	0	1.5	1.5	3	0.0273
41	5	0	0	0	0.0425
42	0	3	0	3	0.0312
43	0	1.5	1.5	1.5	0.0250
44	5	0	0	1.5	0.0216
45	5	3	3	0	0.0248
46	0	0	1.5	1.5	0.0269
47	5	3	0	0	0.0271
48	5	1.5	1.5	1.5	0.0217
49	10	0	3	3	0.0218
50	0	0	1.5	0	0.0571
51	0	1.5	3	3	0.0127
52	5	1.5	1.5	0	0.0398
53	0	1.5	3	1.5	0.0354
54	10	1.5	3	0	0.0216
55	0	3	0	0	0.0490
56	0	3	3	1.5	0.0316
57	5	1.5	1.5	3	0.0307
58	10	0	0	3	0.0172
59	10	3	3	1.5	0.0160
60	10	1.5	1.5	3	0.0273
61	10	3	1.5	0	0.0001
62	10	0	3	0	0.0262
63	0	1.5	0	3	0.0090
64	5	3	0	1.5	0.0367
65	10	0	1.5	3	0.0271
66	10	3	1.5	1.5	0.0267
67	0	3	0	1.5	0.0165
68	5	1.5	0	1.5	0.0347
69	10	1.5	0	1.5	0.0291
70	5	1.5	1.5	1.5	0.0266
71	5	3	1.5	3	0.0122
72	0	3	1.5	3	0.0183
73	0	3	3	3	0.0241
74	10	0	0	1.5	0.0244
75	0	0	3	3	0.0271
76	0	1.5	1.5	0	0.0458
77	5	1.5	1.5	1.5	0.0286
78	5	1.5	3	0	0.0196

79	0	0	1.5	3	0.0250
80	0	0	0	0	0.0460
81	10	1.5	0	0	0.0327
82	10	0	3	1.5	0.0434
83	10	1.5	1.5	1.5	0.0229
84	5	3	0	3	0.0001
85	5	3	1.5	0	0.0203
86	10	3	0	0	0.0221
87	10	3	1.5	3	0.0207

Annexure 3 (Cellulose Hydrolysis kinetics)

Figure 20 below presents the concentration of product Resorufin Vs time which was corrected by Calibration curves. As can be seen the product concentration decreases after reaching a maximum which is predicted to be caused by the decay of fluroscence. Figure 21 represents the relation between rate of change of product with time Vs Product which is linear meaning that product concentration decreases exponentially with time.

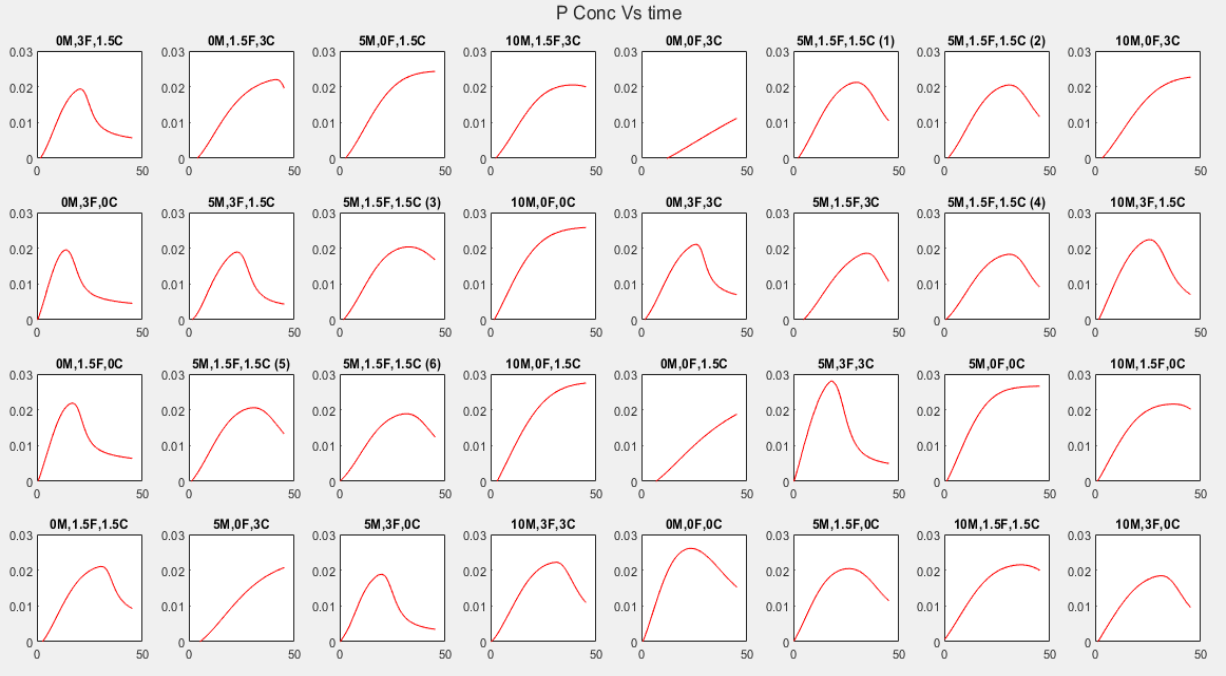

Figure 20: Concentration of product Resorufin Vs time

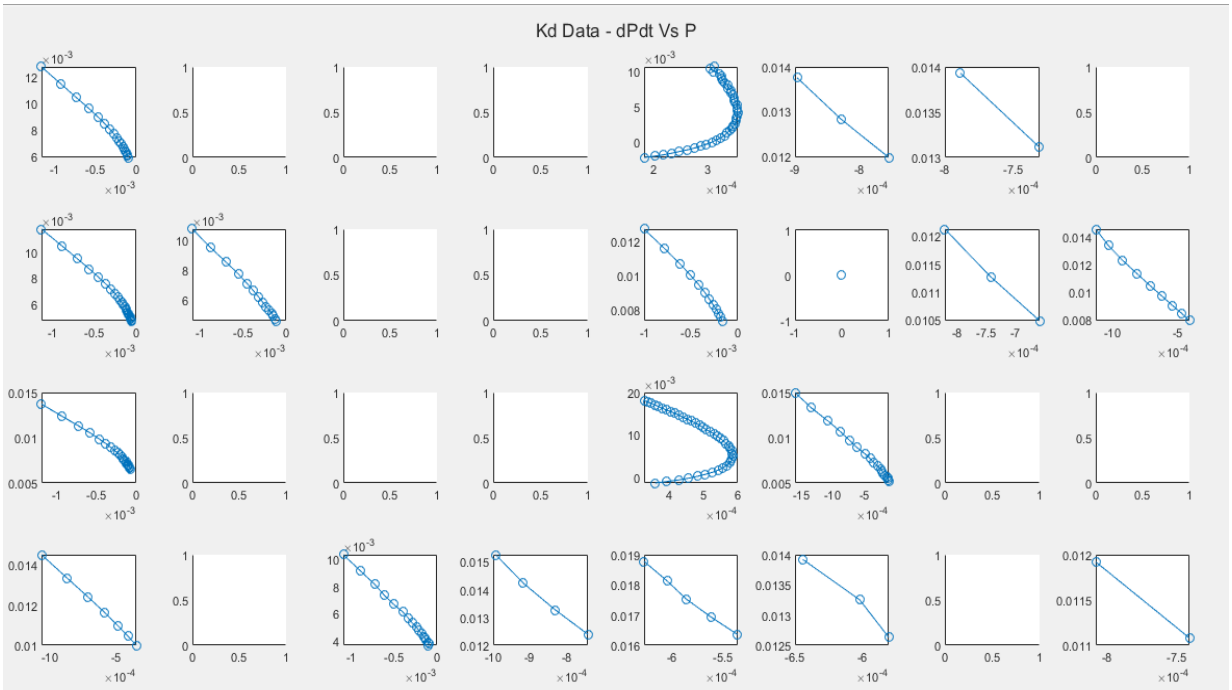

Figure 21: Rate of change of product concentration with time (dP/dt Vs P concentration)

Annexure 4 (Preliminary test for Proteins Hydrolysis – Raw Results)

Figure 22 shows the change in fluorescence with time for protease assay with maximum melanoidins concentration of 10mM and metals Fe^{3+} and Cu^{2+} concentration of 3mM. No increase in fluorescence is observed in presence of metals indicating complete inhibition of enzyme in presence of metals. However, in presence of melanoidins concentration of 5mM hydrolysis of protein does take place to some extent.

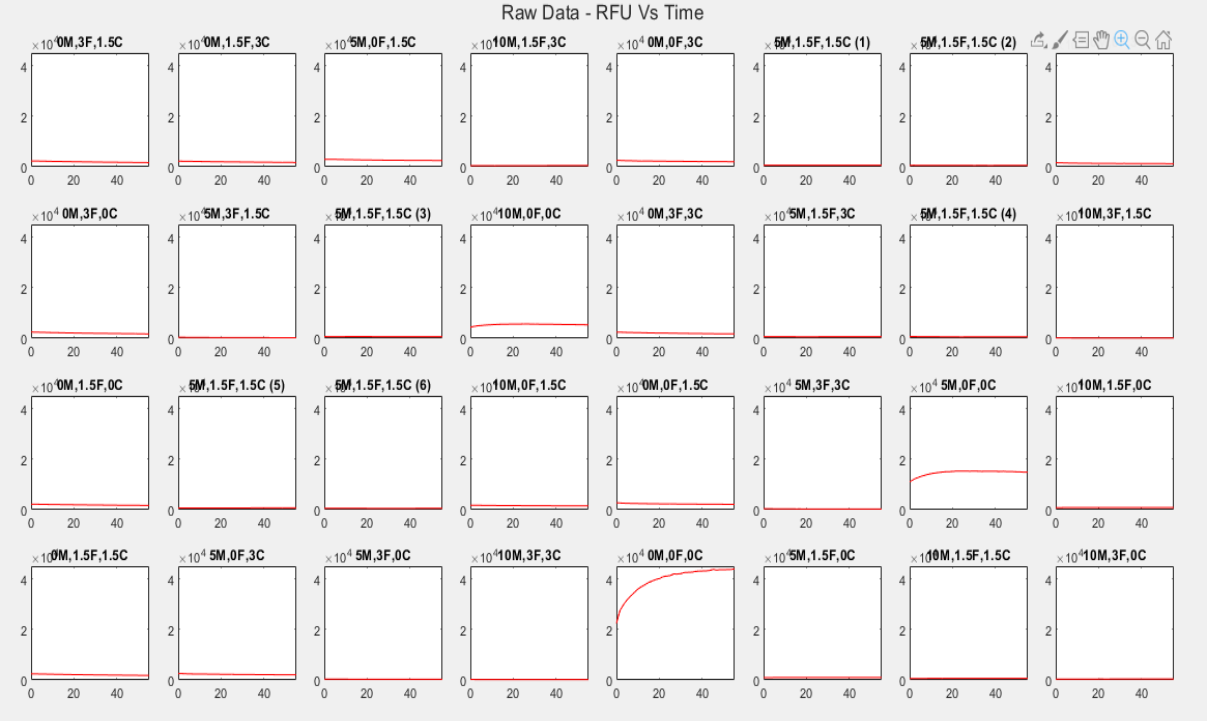

Figure 22: Change in fluorescence with time for protease assay with maximum melanoidins concentration of 10mM and metals Fe^{3+} and Cu^{2+} concentration of 3mM

Annexure 5 (MATLAB Code for Michalis-Menten Kinetics)

```
global y0 Vm Enz_0 Sub_0 kd
yield = 1;                  %Yield enzyme/substrate (to adjust initial
conditions)
Enz_0 = 0.7;                %Initial enzyme
Sub_0 = 0.025;              %Initial substrate
Ksdata = [0.01 0.0007 0.0006 0.0005 0.005 0.003 0.003 0.001...
    0.004 0.008 0.003 0.0003 0.013 0.0007 0.006 0.0007...
    0.003 0.001 0.001 0.0005 0.01 0.01 0.002 0.002...
    0.01 0.001 0.012 0.003 0.001 0.005 0.0001 0.0009];
MMP = zeros(46,32);
MMS = zeros(46,32);
FinKs = zeros(32,1);
for i = 1:b
    Vm = Vmax (i,1);
    p0 = Pconc(1,i);
    Ks0 = Ksdata(1,i);
    Ks = Ksdata(1,i);
    tspan=linspace(0,45.2,46); %time in seconds
    ODE_Sol = ode45(@(t,p)product(t,p,Ks0), time, p0);     % Run the ODE
    simY = deval(ODE_Sol, time);       % Evaluate the solution at the
experimental time steps
    myObjective = @(x) objFcn(x, time, Pconc(:,i),time,p0);
    lb = 0;
    ub = 0.25;
    bestc = lsqnonlin(myObjective, Ks0, lb, ub);
    FinKs (i,1) = bestc;
    ODE_Sol = ode45(@(t,p)product(t,p,bestc), time, p0);
    bestY = deval(ODE_Sol, time);
    for j= 1:46
        MMP(j,i) = simY (1,j);
        MMS(j,i) = bestY (1,j);
    end
end

% Figure 5:MM (P & S Vs time)
figure (5)
ax=tiledlayout(4,8);
title(ax,'P Vs time')
for i=1:32
    nexttile
    plot(time, Pconc(:,i),'-r')
    hold on;
    plot(time, MMP(:,i),'-g')
    hold on;
    plot(time, MMS(:,i),'-b')
    ylim([0,0.03]);
    xlim([0,50]);
    title(wells(i))
 end

function y = product(t, p, Ks)

global Vm Enz_0 Sub_0 kd

% y = Vm * (Sub_0 - p)/(Ks + (Sub_0 - p));
y = Vm * (Sub_0 - p)*Enz_0/(Ks + (Sub_0 - p)) + kd * p;

function ksdata = objFcn(x,t,Pconc,time,p0)
```

```
ODE_Sol = ode45(@(t,p)product(t,p,x), time, p0);
simY = deval(ODE_Sol, t);

ksdata = simY-Pconc;
```

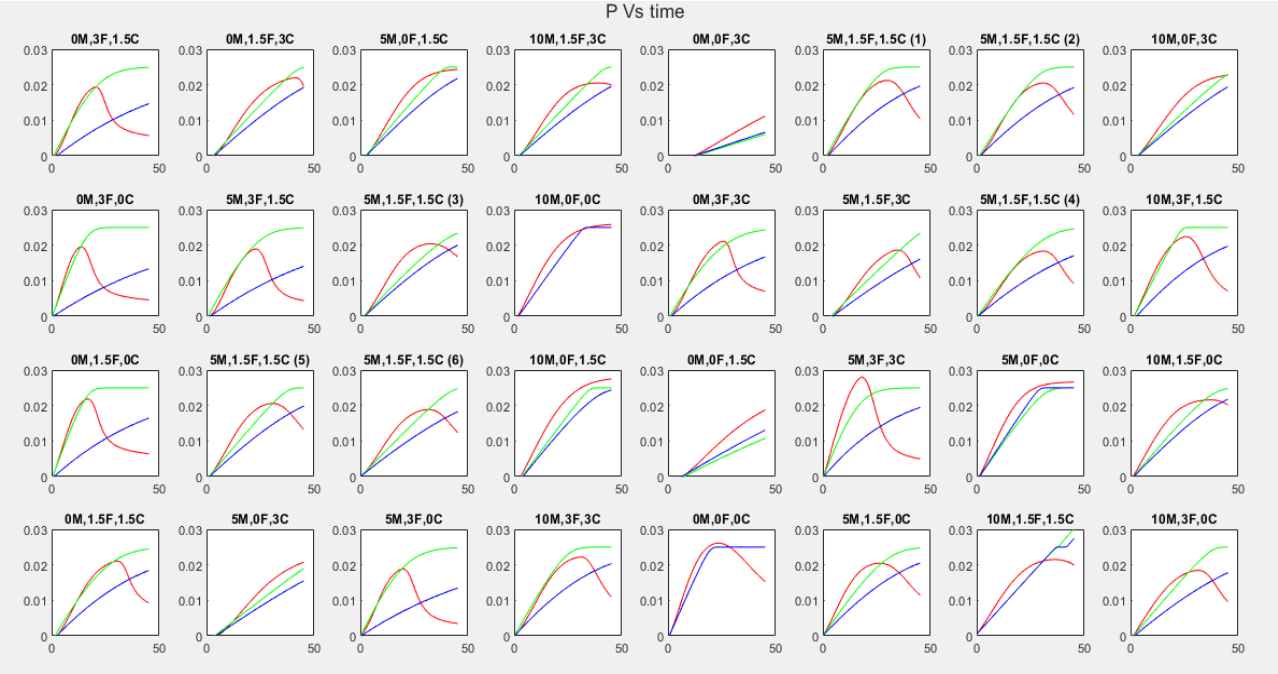

Figure 23: The red line represents the experimental data, Green line represents the solved ODE for Michalis-Menten kinetics and Blue line represents the non-linear fit curve to solve for Ks.